Analysis of the Spin-Polarized Electron Spin Echo of the [$P_{700}^{+}A_1^{-}$] Radical Pair of Photosystem I Indicates That Both Reaction Center Subunits Are Competent in Electron Transfer in Cyanobacteria, Green Algae, and Higher Plants†

Stefano Santabarbara,*,‡,§ Ilya Kuprov,|| P. J. Hore,|| Antonio Casal,‡,§ Peter Heathcote,‡ and Michael C. W. Evans*,§

School of Biological and Chemical Sciences, Queen Mary, University of London, Mile End Road, London E1 4NS, United Kingdom, Department of Biology, University College London, Gower Street, London WC1E 6BT, United Kingdom, and Department of Chemistry, University of Oxford, Physical and Theoretical Chemistry Laboratory, South Parks Road, Oxford OX1 3QZ, United Kingdom

Received February 16, 2006; Revised Manuscript Received April 1, 2006

ABSTRACT: The decay of the light-induced spin-correlated radical pair [$P_{700}^{+}A_1^{-}$] and the associated electron spin echo envelope modulation (ESEEM) have been studied in either thylakoid membranes, cellular membranes, or purified photosystem I prepared from the wild-type strains of *Synechocystis* sp. PCC 6803, *Chlamydomonas reinhardtii*, and *Spinaceae oleracea*. The decay of the spin-correlated radical pair is described in the wild-type membrane by two exponential components with lifetimes of 2−4 and 16−25 μs. The proportions of the two components can be altered by preillumination of the membranes in the presence of reductant at temperatures lower than 220 K, which leads to the complete reduction of the iron−sulfur electron acceptors F_A, F_B, and F_X and partial photoaccumulation of the reduced quinone electron acceptor A_{1A}^{-}. The "out-of-phase" (OOP) ESEEM attributed to the [$P_{700}^{+}A_1^{-}$] radical pair has been investigated in the three species as a function of the preillumination treatment. Values of the dipolar (*D*) and the exchange (*J*) interactions were extracted by time-domain fitting of the OOP-ESEEM. The results obtained in the wild-type systems are compared with two site-directed mutants of *C. reinhardtii* [Santabarbara et al. (2005) *Biochemistry 44*, 2119−2128], in which the spin-polarized signal on either the PsaA- or PsaB-bound electron transfer pathway is suppressed so that the radical pair formed on each electron transfer branch could be monitored selectively. This comparison indicates that when all of the iron−sulfur centers are oxidized, only the echo modulation associated with the A branch [$P_{700}^{+}A_{1A}^{-}$] radical pair is observed. The reduction of the iron−sulfur clusters and the quinone A_1 by preillumination treatment induces a shift in the ESEEM frequency. In all of the systems investigated this observation can be interpreted in terms of different proportions of the signal associated with the [$P_{700}^{+}A_{1A}^{-}$] and [$P_{700}^{+}A_{1B}^{-}$] radical pairs, suggesting that bidirectionality of electron transfer in photosystem I is a common feature of all species rather than being confined to green algae.

Photosystem I (PS I)[1] catalyzes the oxidation of plastocyanin on the lumenal side of the thylakoid membrane and the reduction of ferredoxin on the stromal side (*1*). The reaction center of PS I is a heterodimer of the PsaA and PsaB proteins which coordinate about 100 chlorophyll (Chl) *a* and 30 β-carotene molecules and most of the electron transfer cofactors. The crystallographic structure of PS I from both cyanobacteria (*2*) and higher plants (*3*) has been solved to medium-high resolution, and the electron transfer cofactors have been resolved. The crystal structures show that the electron transfer chain is symmetrically arranged with respect to the axis perpendicular to the membrane plane (*2*, *3*). The structures of the cyanobacterial and higher plant photosystems do not show notable differences in the arrangement of the cofactors, implying that the electron transfer chain is conserved during evolution. The photochemical reactions in PS I take place from the first singlet excited state of the primary electron donor P_{700}, which is a Chl *a*−Chl *a*′ heterodimer. The electron is then transferred to the primary acceptor A_0, a Chl *a* molecule unusually coordinated by a methionine residue, and then to a tightly bound phylloquinone molecule (A_1). The terminal acceptors in PS I are a series of [4Fe-4S] clusters, F_X, F_A, and F_B, which then transfer the electrons to the diffusible carrier, ferredoxin.

Functional and structural evidence has pointed to the possibility that both electron transfer chains, coordinated by either the PsaA or the PsaB subunit, could be photochemically competent. This is often referred to as the bidirectional electron transfer model. Even though evidence in favor of

† This work was supported by grants from the U.K. Biotechnology and Biological Sciences Research Council (BBSRC) (CO0350, CO7809, and B18658), a European Union TMR programme (Contract FMRX-CT98-0214), and a studentship (to I.K.) from the Scatcherd European Foundation and the Hill Foundation.

* To whom correspondence should be addressed. S.S.: phone, +44 2078 824124; fax, +44 2089 835489; e-mail, s.santabarbara@qmul.ac.uk. M.C.W.E.: e-mail, mike.evans@ucl.ac.uk.

‡ Queen Mary, University of London.

§ University College London.

|| University of Oxford.

[1] Abbreviations: PS I, photosystem I; P_{700}, photosystem I primary donor; A_1, phylloquinone acceptor; F_X, iron−sulfur cluster X; EPR, electron paramagnetic resonance; CW, continuous wave; ESE, electron spin echo; ESEEM, electron spin echo envelope modulation; OOP-ESEEM, out-of-phase ESEEM of the flash-induced signal in PS I.

10.1021/bi060330h CCC: $33.50
Published on Web 05/19/2006

functionality of both branches in PS I has been presented (*4*−*10*), and there is general agreement that the PsaA subunit binds a competent electron transfer chain (*4*−*17*), the function of the PsaB-bound electron transfer chain in some organisms, particularly cyanobacteria, is still a matter of debate (*13*−*17*).

The reoxidation kinetics of A_1^- forward electron transfer are biphasic and are described by two lifetimes of about 10−20 and 150−200 ns (*8*, *9*, *18*, *19*). The first evidence for two distinct rates of oxidation of A_1^- was obtained in isolated PS I particles and was originally interpreted as an artifact induced by the detergents employed during PS I purification (*18*, *19*). Joliot and co-workers (*8*, *9*) have subsequently shown that A_1^- reoxidation is biphasic in intact cells of unicellular algae. On the basis of mutagenesis studies of the phylloquinone binding pocket, the slow ∼200 ns component was assigned to the reoxidation rate of the PsaA-bound A_{1A} phyllosemiquinone (*6*, *9*, *11*−*16*, *18*), while the fast ∼20 ns component was assigned to the reoxidation rate of the PsaB-bound A_{1B} (*9*). Moreover, in site-directed mutants of *Chlamydomonas reinhardtii* in which the hydrogen-bonding residue to A_0 has been targeted on both reaction center subunits, the relative amplitudes the two phases of A_1^- are altered, but the lifetime of the reoxidation phase is unchanged compared to the wild type (*20*). The observation that the amplitude of the fast phase of the phyllosemiquinone reoxidation is strongly reduced when the A_{0B} binding site is mutated and the slow phase is quenched when the A_{0A} binding site is modified provides additional support for the assignment of two reoxidation phases to the electron transfer reactions taking place on both reaction center subunits (*20*). The reoxidation kinetics of A_1^- are also biphasic in whole cells of *Synechocystis* sp. PCC 6803 mutants with altered carotenoid composition (*21*) and are characterized by similar lifetime components similar to those measured in *C. reinhardtii*. Biphasic reoxidation rates were also reported for isolated PS I preparations from *Synechocystis* sp. PCC 6803 (*22*). The authors were able to determine different temperature dependences for the two phyllosemiquinone reoxidation phases, one which is markedly temperature dependent, attributed to the PsaA-bound phylloquinone reactions, and one which is essentially temperature independent, attributed to the PsaB phylloquinone reactions (*22*).

On the other hand, the effect of the deletion of the PsaF subunit (*13*) and of site-directed symmetric mutations of the A_0 axial donor ligand to a leucine (*15*, *16*) on the room temperature spin-polarized EPR (electron paramagnetic resonance) signal of the radical pair $[P_{700}^+A_1^-]$ in *Synechocystis* has been interpreted in terms of a very asymmetrical electron transfer in favor of the PsaA branch. The PsaB subunit is argued to contribute, if at all, a maximum of 10−15% of the total electron transfer in this organism (*17*).

Below 100 K only about half of the PS I centers are capable of forward electron transfer from A_1^- to F_X (*19*, *23*). In this condition it is possible to monitor the recombination reaction of the radical pair, either by optical (*19*, *23*−*25*) or magnetic resonance techniques (refs *4*, *6*, *7*, and *26* and references cited therein). The decay lifetime of the electron spin-polarized signal associated with the spin-correlated $[P_{700}^+A_1^-]$ radical pair reflects contributions from charge recombination and from loss of correlation within the radical pair due to spin−lattice relaxation. When the iron−sulfur electron acceptors are oxidized, essentially a single rate of decay (∼20 μs) for this signal is observed (*4*, *6*, *7*, *26*−*28*). The electron spin echo decaying at this rate arises from $[P_{700}^+A_1^-]$ formed on the PsaA side of the reaction center (*4*, *6*, *7*, *26*−*28*). Following reduction of the iron−sulfur acceptors this decay becomes biphasic in thylakoids prepared from *C. reinhardtii* and *Synechocystis* sp. PCC 6803 (*4*, *6*, *7*), showing lifetimes of 2−4 and 15−20 μs. It was suggested that the 2−4 μs recombination rate was associated with the PsaB electron transfer branch and the 15−20 μs with the PsaA branch (*4*). The effect of mutation of the methionine A_0 axial ligand to histidine in *C. reinhardtii* thylakoids, which allows selective observation of the two components of the $[P_{700}^+A_1^-]$ decay, supports this proposal (*6*, *7*).

The possibility of selectively monitoring the two components of the $[P_{700}^+A_1^-]$ decay has been exploited to investigate the modulation of the out-of-phase (OOP) spin echoes (*7*), which provides information about the distance between the partners within the radical pair (*29*−*36*). Theoretical studies (*29*−*34*) have shown that the OOP-ESEEM is not dominated by hyperfine interactions, as is typical of in-phase echoes, but by the interelectron dipolar (*D*) and exchange (*J*) interactions. Because the partners in the radical pair, P_{700}^+ and A_1^-, are separated by about 25 Å (*2*, *3*, *7*, *33*−*36*), $|D|$ is about 2 orders of magnitude larger than $|J|$ (e.g., refs *37* and *38*). The dipolar term therefore dominates the OOP-ESEEM time dependence. Experimental determination of the value of *D* allows accurate determination of the distance between the centers of electron spin density in the radical pair (*33*−*38*).

Investigation of the OOP-ESEEM in wild type and the PsaA-M684H and PsaB-M664H mutants of *C. reinhardtii* has led to the conclusion that two different radical pairs are observed in the mutants (*7*), characterized by $D = -194.84 \pm 0.46$ μT, $J = 4.59 \pm 0.22$ μT and $D = -171.02 \pm 0.29$ μT, $J = 0.80 \pm 0.12$ μT for PsaA-M684H and PsaB-M664H, respectively. This results in distance estimates for $P_{700}^+-A_{1A}^-$ and $P_{700}^+-A_{1B}^-$ which agree with the crystal structures when the asymmetric spin distribution of the primary donor P_{700}^+ chlorophyll dimer is considered (*39*−*42*). In the wild type, a mixed situation is observed which originates under appropriate conditions from almost equally weighted contributions of radical pairs formed on the two reaction center subunits (*6*, *7*).

It appears that some of the controversy regarding the directionality of electron transfer in PS I originates from the use of different spectroscopic techniques, different organisms, and, in some cases, different choices of axial ligand substitution (*4*−*10*, *13*−*17*). To try to address the question of whether different organisms show different proportions of electron transfer on the two branches, we have recorded and analyzed the decay and the ESEEM of the polarized electron spin echo (ESE) signal associated with the radical pair $[P_{700}^+A_1^-]$ at 100 K, in wild-type thylakoids or purified PS I, from a cyanobacterium (*Synechocystis* sp. PCC 6803), a green alga (*C. reinhardtii*), and a higher plant (*Spinaceae oleracea*). The effect of the reduction of F_X and partial reduction of A_1 is investigated and compared with the previously reported effect of site-directed mutation of the A_0 axial ligand on each of the reaction center subunits of PS I in *C. reinhardtii*. The results are interpreted in terms

of two different radical pairs populated on either the PsaA or the PsaB subunit of the PS I reaction center in all of the organisms investigated. This is in agreement with previous results obtained in the green algae *C. reinhardtii* and indicates that bidirectionality is a general rather than a species-specific feature of PS I electron transfer.

MATERIALS AND METHODS

Cell Growth and Preparation of Thylakoid Membranes. *C. reinhardtii* was grown on acetate supplemented medium (TAP), and thylakoids were prepared as described by Diner and Wollman (*43*) with minor modifications (*7*). The prepared thylakoids were resuspended at a concentration equivalent to 2 mg mL^{-1} Chl in buffer containing 50 mM KHepes, 10 mM NaCl, 5 mM $MgCl_2$, and 100 mM sorbitol at pH 8. *Synechocystis* sp. PCC 6803 was grown, and cellular membranes were prepared as in ref *44*. Thylakoid membranes from spinach were prepared as previously described (*45*) and resuspended in a 100 mM Tricine, 10 mM NaCl, 5 mM $MgCl_2$ (pH 7.8) buffer at a Chl concentration of 2 mg mL^{-1}. A PS I preparation was obtained by the digitonin method as previously described (*46*) with minor modifications. The thylakoids were suspended in a 100 mM Tricine, 0.1 M sorbitol, 10 mM NaCl, 5 mM $MgCl_2$ (pH 7.8) buffer and solubilized for 30 min in a 0.5% w/v digitonin solution at a Chl concentration equivalent to 500 μg mL^{-1}. The membrane fraction 144000*g* pellet resulting from differential centrifugation is denoted as PS I. Sodium ascorbate, 20 mM (*47*), and sodium dithionite, 11.5 mM (*7*), reduced samples were prepared as previously described.

Preillumination Treatments at Cryogenic Temperature. The samples, incubated with 11.5 mM sodium dithionite at pH 8 (100 mM Tricine, 10 mM NaCl, 5 mM $MgCl_2$ buffer) in a 3 mm i.d. quartz EPR tube, at a chlorophyll concentration equivalent to 2 mg mL^{-1}, were placed in a cylindrical quartz Dewar vessel (11 cm diameter) containing ethanol and solid CO_2 in pellets. Photoreduction of the iron−sulfur center F_X and photoaccumulation of A_1 were performed at 205 K. To obtain homogeneous illumination of the sample, the ethanol/CO_2 bath was left to equilibrate with the dry ice deposited on the bottom of the vessel, and the temperature was monitored by a calibrated K-type thermocouple (Hanna Instruments, model LPK2). Illumination was provided by a halogen 1000W projector lamp (Reflecta, model flectalux GLS1008) placed 11 cm from the center of the Dewar. The incident white light was filtered though a 4 cm thick water-filled glass container to remove infrared and ultraviolet light. The photon flux density of the white light irradiation at the sample level is 3650 μE m^2 s^{-1} and was measured by a Li-COR light meter (model Li-250A), equipped with a Li-193sa quantum sensor.

The reduction of the PS I electron acceptors was routinely monitored by continuous wave (CW) EPR either using a JEOL RX-1 spectrometer, equipped with a resonator which allows illumination of the sample in the EPR cavity (*47*), or in a Bruker Elexsys E 580 spectrometer, at X-band (9.5 GHz, 300 mT). Reduction of $F_{A/B}$ suppresses any irreversible P_{700}^+ oxidation at 10 K (e.g., ref *48*). However, reversible P_{700}^+ oxidation can still be observed under continuous illumination, which is due to electron transfer between P_{700}^+ and F_X^- (e.g., refs *48* and *49*). Preillumination of dithionithe-reduced samples at 205 K for 5 min suppresses the irreversible and more than 95% of the reversible oxidation of P_{700}^+ due to F_X reduction (e.g., ref *49*). However, a small radical signal centered at *g* 2.00 is observed without illumination in the resonator. Based on its line shape the signal is attributed to the A_{1A}^- radical, in agreement with previous results (e.g., refs *46*, *50*, and *51*). These conditions are chosen as they result in an almost complete reduction of F_X but minimize A_1^- photoaccumulation (*7*). The kinetics of A_{1A}^- photoaccumulation at pH 8 was followed in the Bruker Elexsys E 580 spectrometer, equipped with a super-high Q (SHQ) cylindrical resonator. The spectra were acquired at 50 K with a field modulation of 0.1 mT and a microwave power of 10 μW to avoid band-shape distortions. The spin concentration was quantified by double integration of the first-harmonic EPR spectrum. The data were normalized to the amount of P_{700}^+ induced by illumination at 77 K of a matching sodium ascorbate (20 mM) incubated sample.

Time-Resolved Electron Paramagnetic Resonance. The ESEEM time dependence and the decay of the ESE as a function of the delay after laser excitation were measured using a Bruker ESP580 X-band spectrometer equipped with a variable Q dielectric resonator (Bruker EN4118 X-MD-4W), which has previously been described in detail (*7*). The EPR cavity was fitted with an Oxford Instruments CF935 cryostat cooled with liquid nitrogen, with the temperature controlled by an Oxford Instruments ITC-5 controller. Actinic illumination was supplied by an Nd:YAG laser (Spectra Physics DCR-11): 10 ns pulse duration, 20 mJ energy per pulse, and 532 nm wavelength. The acquisition was triggered by the laser Q-switch. Flashes are fired at a frequency of 10 Hz to avoid interference from spin-polarized metastable states (e.g., triplet states and long-lived tertiary radical pairs).

The two-pulse echo sequence consisted of a $\pi/2$ pulse (8 ns) and a refocusing π pulse (16 ns). The ESEEM time dependencies were recorded with an initial echo delay (τ) of 112 ns, incremented with 8 ns steps. The light-induced OOP-ESEEM was recorded by measuring the signal intensity at time $t = \tau$ from the center of the second microwave pulse. The spectrometer time resolution, limited by laser jitter, is ~50 ns.

Corrections for imperfect receiver phase setting and possible contributions from stable radicals generated during the flash-induced ESE experiments were performed as previously described (*7*).

Data Analysis. The time decay of the ESE signal was fitted with a sum of exponential functions using the Levenberg−Marquardt algorithm. The data acquired from samples incubated with sodium ascorbate or sodium dithionite in the dark were analyzed by treating the decay lifetimes and the preexponential amplitudes as free parameters. Data from samples reduced by sodium dithionite and preilluminated at 205 K and at 220 K were fitted simultaneously, constraining the lifetimes to be identical for the two illumination conditions while the amplitudes are allowed to differ. The errors were determined by the variance−covariance matrix method within a confidence interval of 2σ.

The ESEEM model used in this work relies on the following assumptions: point-dipole approximation for the interelectron dipole interaction, fast dephasing/relaxation of two-electron zero-quantum coherence, weak dipolar and exchange coupling (i.e., couplings are much smaller than the

difference in electron Zeeman frequencies of the two radicals), small hyperfine couplings (such that it is permissible to ignore nuclear modulations in the ESEEM signal), and mono-exponential decoherence. A large body of research has indicated the validity of these assumptions for the systems under investigation (ref *7* and references cited therein). The expression for the ESEEM signal can then be obtained analytically:

$$S(\tau) = \frac{2\pi^{3/2} H e^{-\tau/T}}{\sqrt{D\tau}}\left[\sin\left(\frac{2(D+3J)\tau}{3}\right)\mathrm{FrC}\left(2\sqrt{\frac{D\tau}{\pi}}\right) - \cos\left(\frac{2(D+3J)\tau}{3}\right)\mathrm{FrS}\left(2\sqrt{\frac{D\tau}{\pi}}\right)\right]$$

$$\mathrm{FrC}(z) = \int_0^z \cos(\pi u^2/2)\, du$$

$$\mathrm{FrS}(z) = \int_0^z \sin(\pi u^2/2)\, du \qquad (1)$$

where FrC and FrS are Fresnel cosine and sine functions, respectively, D is the dipolar interaction, J is the exchange interaction, T is the relaxation time, H is the amplitude of the echo modulation signal, and angular frequency units are used for all interaction energies. Augmented by a second-order polynomial baseline correction term, eq 1 fits the experimental data extremely well.

Equation 1 does not take into account the presence of the extra electron spin on $F_{A/B/X}^-$ in the reduced samples. As previously discussed (*7*), such effects are very unlikely to be significant, either because the spin evolution resulting from the coupling between $F_{A/B/X}^-$ and P_{700}^+ and/or A_1^- is refocused in the spin echo or because it is averaged out by rapid spin relaxation of $F_{A/B/X}^-$.

Values of the parameters D, J, and T were extracted by a least-squares fit to the experimental data. Where necessary, a frequency-domain signal was obtained by reconstructing the signal during the instrumental dead time using the theoretical fit with subsequent sine Fourier transformation. The error bounds on all parameters were obtained using the Cramer−Rao lower bounds theorem (*34*).

The distance X between the electron spins in the radical pair can be estimated from the value of D (in tesla):

$$D = -[(3g_e\mu_B\mu_0)/(8\pi X^3)] \qquad (2)$$

where g_e is the g-factor of the free electron, μ_B is the Bohr magneton, and μ_0 is the vacuum permeability.

The distances obtained in the point-dipole approximation are between the weighted averages of the spatial distributions of the two unpaired electrons, which are not identical to the separations of the physical centers of the two radicals. However, unless there are significant changes in the spin density distributions of one or both radicals, the distances calculated from eq 2 can reliably be used to compare the separations of spin-correlated radicals in the same or different species.

Global Fitting Analysis of the OOP-ESEEM. The OOP-ESEEM signals recorded for different reduction states of the electron acceptors ($F_{A/B/X}$ and A_1) were also fitted using a linear combination of two OOP-ESEEM functions:

$$S(\tau) = A_1 S_1(\tau) + A_2 S_2(\tau) + g(\tau) \qquad (3)$$

where $g(\tau)$ is a quadratic baseline correction term and $S_i(\tau)$ are described by eq 1 and weighted by the amplitude factors A_i. Several data sets, recorded under different reduction conditions, were fitted simultaneously, constraining D and J to be common to all sets and allowing A_1, A_2, and T to differ between sets.

RESULTS

Time Decay of the [$P_{700}^+A_1^-$] Electron Spin Echo as a Function of the Reduction State of the PS I Electron Acceptors. In sodium ascorbate incubated samples all of the iron−sulfur clusters are initially oxidized (refs *48*, *49*, and *52* and references cited therein). Incubation with sodium dithionite in the dark results in partial reduction of F_A and F_B except in the cellular membranes purified from *Synechocystis* (data not presented). F_X is largely oxidized under these conditions because of its negative redox midpoint potential which is estimated to be in the −(690−730) mV range (*53*−*55*). Preillumination of the samples for 5 min at 205 K abolishes any irreversible light minus dark changes in the CW-EPR spectra, indicating complete reduction of $F_{A/B}$. F_X is almost completely reduced by the brief preillumination at 205 K (*48*, *49*), but some reversible P_{700} oxidation coupled to a partial reduction of F_X is still observed when the CW-EPR spectra are recorded under continuous illumination in the spectrometer resonator (*48*, *49*). Further preillumination of the samples at 205 K at pH 8 results in complete reduction of F_X and the accumulation of a radical species, which can be quantified as reaching one spin per P_{700}^+ and has been attributed to the phyllosemiquinone radical bound to the PsaA reaction center subunit, A_{1A}^- (e.g., refs *5*, *47*, *49*−*51*, *56*, and *57*). The same effect can be obtained by illumination of the samples at 220 K for 10 min, which results in the loss of both reversible and irreversible CW-EPR detectable P_{700} oxidation, indicating full reduction of all three Fe−S clusters (*5*, *47*, *56*, *57*).

Figure 1 shows the decay of the OOP electron spin echo of [$P_{700}^+A_1^-$] in spinach thylakoids. The echo decay has been detected under conditions in which the terminal clusters F_A and F_B are initially oxidized (Figure 1A), mainly reduced (Figure 1B), completely reduced with F_X essentially fully reduced (Figure 1C) and all three iron−sulfur clusters $F_{A/B/X}$ reduced with A_{1A} partially reduced (Figure 1D). The OOP-ESE decay was also measured in thylakoids from *C. reinhardtii*, cellular membranes from *Synechocystis*, and a digitonin PS I preparation from spinach (Supporting Information, Figure S1).

The data recorded for the three different organisms can be fitted under all conditions by a sum of two exponential functions, in agreement with our previous observations for *C. reinhardtii* thylakoids (*7*). The two echo decays obtained for samples containing oxidized F_X and A_{1A} (panels A and B in Figure 1) were fitted separately, while the two obtained for samples in which F_X and A_{1A} were partially or fully reduced (panels C and D in Figure 1) were fitted simultaneously (see Materials and Methods and ref *7* for further details). The results of this fitting are shown in Figure 1 and the parameters reported in Table 1 for the thylakoids purified from *C. reinhardtii*, the cellular membranes from *Synechocystis*, and the PS I preparation from spinach.

We have previously reported that the decay ESE in sodium ascorbate incubated samples, in which F_A and F_B are initially

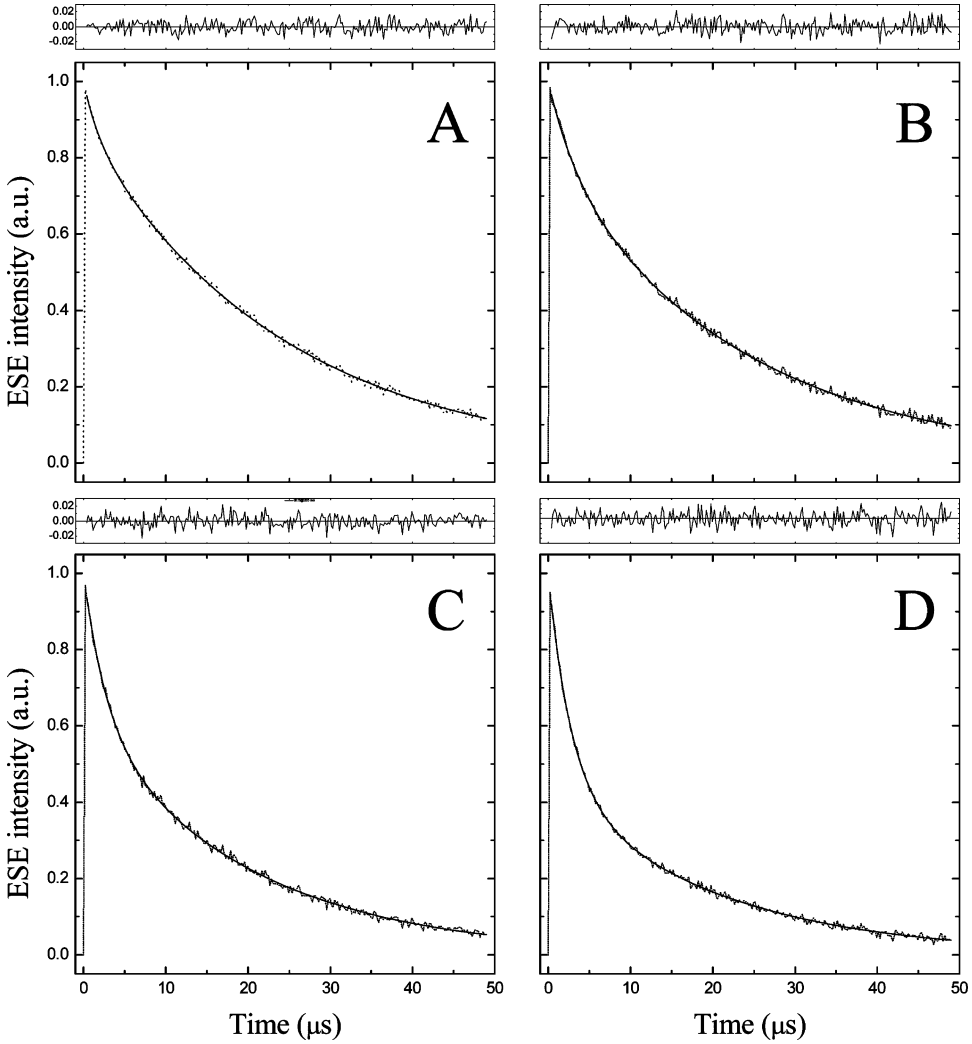

FIGURE 1: Decay of the two-pulse electron spin echo associated with the radical pair $[P_{700}{}^{+}A_1{}^{-}]$ in spinach thylakoids under different reduction states of the electron transfer acceptors of PS I: (A) 20 mM sodium ascorbate, dark-adapted membrane (oxidized $F_{A/B/X}$); (B) 10 mM sodium dithionite, dark-adapted membrane (partially reduced $F_{A/B}$); (C) 10 mM sodium dithionite, 5 min preillumination at 205 K (reduced $F_{A/B/X}$); (D) 10 mM sodium dithionite, 10 min preillumination at 220 K (reduced $F_{A/B/X}$, partially photoaccumulated $A_1{}^{-}$). Experimental conditions: field, 346.4 mT; frequency, 9.75 GHz; temperature, 100 K.

Table 1: Analysis of the Decay of the $[P_{700}{}^{+}A_1{}^{-}]$ Out-of-Phase Electron Spin Echo[a]

	A_1	τ_1 (μs)	A_2	τ_2 (μs)	τ_{av} (μs)
spinach thylakoids					
Asc, dark	0.12 ± 0.1	1.80 ± 0.03	0.86 ± 0.2	24.12 ± 0.1	20.95 ± 0.2
Dit, dark	0.20 ± 0.1	3.32 ± 0.03	0.80 ± 0.2	23.33 ± 0.1	19.32 ± 0.2
Dit, 5 min (205 K)	0.38 ± 0.2	2.74 ± 0.02	0.62 ± 0.2	19.87 ± 0.2	13.36 ± 0.2
Dit, 15 min (220 K)	0.55 ± 0.1	2.74 ± 0.03	0.45 ± 0.2	19.87 ± 0.1	10.45 ± 0.2
spinach PS I enriched membranes					
Asc, dark	0.10 ± 0.1	1.80 ± 0.03	0.90 ± 0.2	19.02 ± 0.1	17.30 ± 0.2
Dit, dark	0.28 ± 0.1	2.72 ± 0.03	0.72 ± 0.2	18.32 ± 0.1	13.95 ± 0.2
Dit, 5 min (205 K)	0.49 ± 0.1	2.52 ± 0.03	0.51 ± 0.2	16.32 ± 0.1	9.56 ± 0.2
Dit, 15 min (220 K)	0.75 ± 0.1	2.52 ± 0.03	0.25 ± 0.2	16.32 ± 0.1	5.97 ± 0.2
C. reinhardtii thylakoids					
Asc, dark	0.14 ± 0.1	1.60 ± 0.03	0.86 ± 0.2	23.12 ± 0.1	20.11 ± 0.2
Dit, dark	0.24 ± 0.1	3.12 ± 0.03	0.76 ± 0.2	22.22 ± 0.1	17.64 ± 0.2
Dit, 5 min (205 K)	0.43 ± 0.2	2.52 ± 0.02	0.57 ± 0.2	19.57 ± 0.2	12.24 ± 0.2
Dit, 15 min (220 K)	0.64 ± 0.1	2.52 ± 0.03	0.33 ± 0.2	19.57 ± 0.1	10.42 ± 0.2
Synechocystis sp. PCC 6803 thylakoids					
Asc, dark	0.12 ± 0.1	1.80 ± 0.03	0.88 ± 0.2	28.22 ± 0.1	25.05 ± 0.2
Dit, dark	0.05 ± 0.1	4.12 ± 0.03	0.95 ± 0.2	27.73 ± 0.1	26.55 ± 0.2
Dit, 5 min (205 K)	0.28 ± 0.1	3.21 ± 0.03	0.72 ± 0.2	26.84 ± 0.1	20.22 ± 0.2
Dit, 15 min (220 K)	0.50 ± 0.1	3.21 ± 0.03	0.50 ± 0.2	26.84 ± 0.1	15.03 ± 0.2

[a] Results of fitting the decay of the electron spin echo associated with the spin-polarized radical pair $[P_{700}{}^{+}A_1{}^{-}]$ in isolated thylakoids from several species with different extents of reduction of the electron acceptors of photosystem I. Abbreviations: Asc, sample incubated in 20 mM sodium ascorbate buffered solution at pH 8; Dit, sample incubated in 11.5 mM sodium dithionite buffered solution at pH 8. The temperature in parentheses indicates the preillumination conditions. All of the data were recorded at 100 K. The data were fitted by a linear combination of exponential functions: $y(t) = \sum_{i=1}^{n} A_i e^{-t/\tau_i}$. The average decay lifetime is defined as $\tau_{av} = \sum_{i=1}^{n} A_i \tau_i / \sum_{i=1}^{n} A_i$.

oxidized, is monoexponential (*4*, *6*) and is characterized by a lifetime of ~20−24 μs. The improved signal-to-noise ratio of the data reported here allows us to distinguish a second component with a lifetime of ~1.5 μs. The precise value of this lifetime depends on the species (Table 1). The ~20−24 μs contribution accounts for more than 80% of the initial amplitude and is the component that was detected and characterized in previous reports (*4*, *6*). It is likely that the ~1.5 μs phase reflects the decay of the net P_{700}^+ polarization in a fraction of centers that are able to perform forward electron transfer to the oxidized $F_{A/B}$ clusters. A decay component of ~1.4 μs has been previously reported in time-resolved direct detection EPR studies at room temperature and attributed to one of the possible [$P_{700}^+FeS^-$] radical pairs (refs *13*, *14*, and *23* and references cited therein).

In the samples in which F_A and F_B only have been reduced, the decay is also biexponential and dominated by an ~20 μs decay component. However, the second component has an ~2−3 μs lifetime in these samples (Table 1), in agreement with previous reports (*4*, *6*, *7*). After complete reduction of the iron−sulfur centers by preillumination at 205 K, the OOP echo is characterized by two almost equally weighted exponential components with lifetimes of 2−3 and 15−18 μs. Further preillumination does not modify these lifetimes but does alter their relative weights.

Figure 2 shows the photoaccumulation time dependence of the initial amplitudes of the components of the ESE signal decay in the spinach thylakoid and *Synechocystis* cellular membranes at 205 K. The maximum signal amplitude is detected, both for spinach and for *Synechocystis* preparations, after 5 min of illumination at 205 K, i.e., the conditions that have been found to maximize the reduction of F_X with minimal reduction of A_{1A} (*7*). Prolonged illumination reduces the initial amplitude of the 15−18 μs component, while the amplitude of the 2−3 μs component is essentially unaltered. The dependence of the calculated average lifetime on the photoaccumulation length is also presented in Figure 2 and clearly shows the increasing relative contribution of the 2−4 μs component to the initial intensity of the electron spin echo.

Figure 3 shows that the amplitude associated with the "slow" 15−20 μs component decreases linearly as the amount of the photoaccumulated A_{1A}^- radical at 205 K (determined by CW-EPR at X-band) increases. Similar results were obtained in *C. reinhardtii* thylakoids and in a spinach PS I digitonin preparation (Supporting Information, Figure S2). The suppression of the ~15−20 μs component appears to be more rapid in spinach and *C. reinhardtii* than in *Synechocystis* and is even more rapid in the PS I digitonin preparation. These differences in the kinetics of A_{1A}^- photoaccumulation can be attributed either to different redox properties of the phylloquinone molecule in different species (i.e., cyanobacteria compared to higher plants and green algae) or to the purification procedure that might either alter the redox midpoint potential or make the quinone more accessible to the chemical reductant. The latter would be consistent with the observation that some detergents (e.g., Triton X-100) alter the hyperfine couplings in the photoaccumulated A_{1A}^- (*57*). It has also been shown that some of the minor subunits located close to the A_{1A} binding site alter the susceptibility of this quinone to detergents (*17*, *24*). Another factor which might influence the photoaccumulation kinetics and temperature dependence is the rate of electron donation of the chemical reducing agent (dithionite) to P_{700}^+ in the different preparations, as it is chemical reduction of the primary donor cation which makes photoaccumulation possible. At present we are not able to discriminate between these possibilities. It is possible that both phenomena contribute to the differences in photoaccumulation characteristics between different species and preparations.

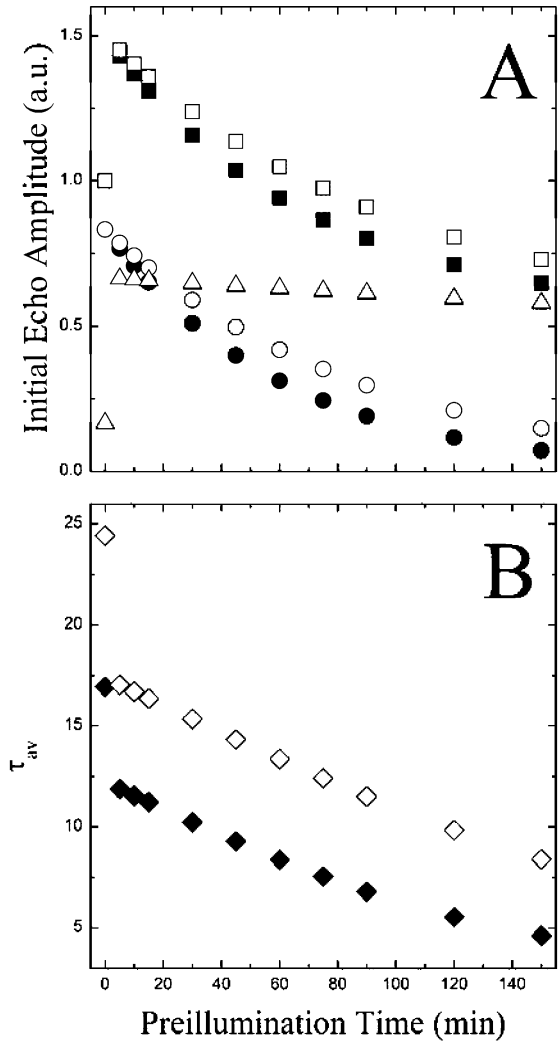

FIGURE 2: (A) Relationship between the photoaccumulation treatment time (in the presence of 11.5 mM sodium dithionite) and the amplitudes of the decay components of the ESE associated with the [$P_{700}^+A_1^-$] radical pair in thylakoid membranes from spinach (solid symbols) and *Synechocystis* sp. PCC 6803 (open symbols). Key: squares, initial amplitude at τ_0; circles, amplitude of the slow 16−20 μs component of the ESE decay; triangles, amplitude of the fast 2−4 μs component of the ESE decay. The decay components have been normalized to the maximum of the total initial amplitude to allow simple comparison. (B) Relation between the photoaccumulation treatment time and the average lifetime of the [$P_{700}^+A_1^-$] ESE. Key: solid diamonds, spinach thylakoids; open diamonds, *Synechocystis* sp. PCC 6803 thylakoids. Experimental conditions are as in the legend of Figure 1.

Analysis of the OOP-ESEEM Associated with the [$P_{700}^+A_1^-$] Radical Pair as a Function of the Reduction State of the Electron Acceptors in PS I. Figure 4 displays the OOP-ESEEM detected in thylakoids and the digitonin PS I preparation from spinach. The following conditions were studied: ascorbate incubation (initially oxidized $F_{A/B}$), dithionite incubation (partially reduced $F_{A/B}$), 5 min photoaccumulation at 205 K in the presence of dithionite (largely

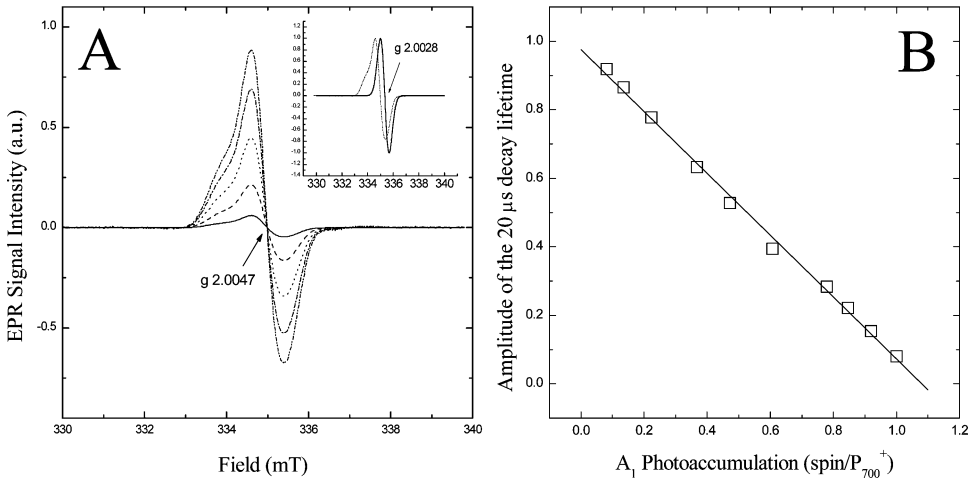

FIGURE 3: (A) Kinetics of A_{1A}^- photoaccumulation in spinach thylakoid membranes incubated with 11.5 mM sodium dithionite at pH 8 and 205 K monitored by CW-EPR. Preillumination time: 5 min (solid line), 15 min (dashed line), 45 min (dotted line), 90 min (dash−dotted line), 120 min (dash−dot−dotted line). The insert compares the signal obtained for a matching sample incubated with 20 mM sodium ascorbate at pH 8, illuminated a 77 K (solid line) attributed to P_{700}^+, with the spectrum obtained after 120 min of preillumination at 205 K. Experimental conditions: microwave power, 10 μW; field modulation, 0.1 mT; temperature, 45 K. All of the spectra corrected are plotted on a correct field scale, using an arbitrary frequency of 9.4 GHz. Also shown are the calculated *g* values for both radical species. (B) Correlation between the photoaccumulation of the A_{1A}^- radical at 205 K, quantified by double integration of the CW-EPR spectra, and the decrease in the amplitude of the slow 16−20 μs component of the ESE decay of $[P_{700}^+A_1^-]$ in spinach thylakoid membranes monitored at 100 K.

reduced F_X), and 15 min photoaccumulation at 220 K in the presence of dithionite (fully reduced F_X and partially reduced A_1). The OOP-ESEEM recorded for *C. reinhardtii* thylakoid samples subjected to identical pretreatments are shown in Figure 5.

In cellular membranes purified from *Synechocystis* sp. PCC 6803 the OOP-ESEEM recorded in ascorbate and dithionite dark-reduced samples are essentially identical ($D = -167.15 \pm 0.41$ μT, $J = 1.03 \pm 0.20$ μT and $D = -167.20 \pm 0.35$ μT, $J = 1.05 \pm 0.15$ μT). Nevertheless, brief illumination at 205 K produces a change in the modulation of the OOP-ESEEM, which is amplified by illumination at 220 K for 15 and 30 min (Figure 6).

The distance between the two electrons of a spin-correlated radical pair can be obtained from the value of the interelectron dipolar interaction energy (eq 2). To obtain this parameter, we have fitted eq 1 to the time-domain OOP-ESEEM data recorded under the different reduction conditions. The resulting fits and their extrapolation into the spectrometer dead time are presented in Figures 4−6. The sine Fourier transforms (SFT) of the time-domain ESEEM and the fits are also presented in Figures 5 and 6. As one can see, all of the features in the frequency-domain spectra are correctly described by the transformed fit functions. Minor discrepancies are due to nuclear modulations which have been neglected in eq 1. The fit parameters are listed in Table 2.

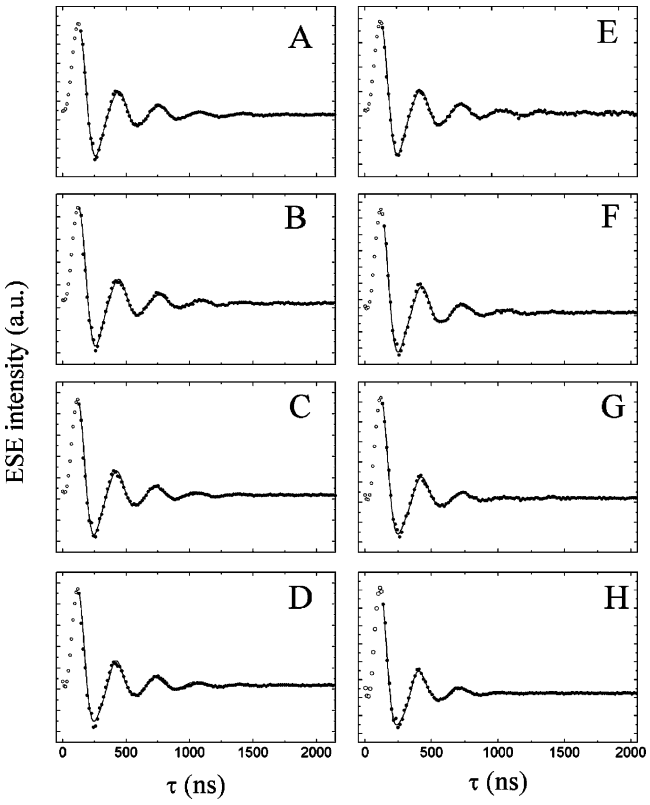

FIGURE 4: Time dependence of the out-of-phase ESEEM of the spin-correlated radical pair $[P_{700}^+A_1^-]$ in spinach thylakoids (A−D) and PS I enriched membranes (E−H). Solid circles are the experimental results; solid lines are the fits according to eq 3; open circles are the extrapolation to $\tau = 0$. Panels: (A, E) 20 mM sodium ascorbate, dark-adapted membrane (oxidized $F_{A/B/X}$); (B, F) 10 mM sodium dithionite, dark-adapted membrane (partially reduced $F_{A/B}$); (C, G) 10 mM sodium dithionite, 5 min preillumination at 205 K (reduced $F_{A/B/X}$); (D, H) 10 mM sodium dithionite, 15 min preillumination at 220 K (reduced $F_{A/B/X}$, partially photoaccumulated A_1^-). Experimental conditions: field, 346.4 mT; mictowave frequency, 9.71 GHz; temperature, 100 K.

DISCUSSION

The results presented here show that progressive reduction of the PS I electron transfer acceptors influences the decay of the $[P_{700}^+A_1^-]$ radical pair ESE, which exhibits biphasic kinetics after reduction of the bound Fe-S centers $F_{A/B}$ and F_X.

The values of the spin−spin interaction energies derived from the fitting of the time-domain ESEEM also change, indicating a dependence on the redox state of the electron

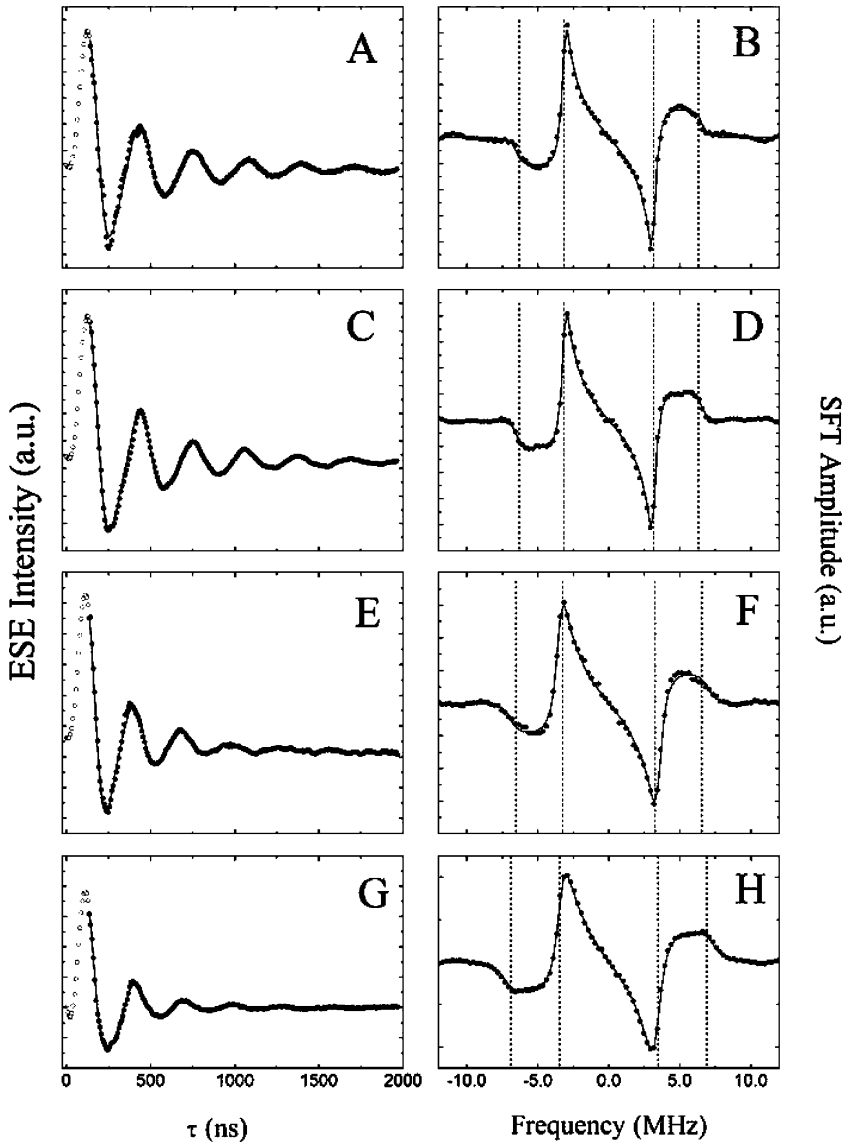

FIGURE 5: Time dependence of the out-of-phase ESEEM of the spin-correlated radical pair [$P_{700}^{+}A_1^{-}$] in *C. reinhardtii* thylakoids. Solid circles are the experimental results; solid lines are the fits according to eq 1; open circles are the extrapolation to $\tau = 0$. Panels: (A) 20 mM sodium ascorbate, dark-adapted membrane (oxidized $F_{A/B/X}$); (C) 10 mM sodium dithionite, dark-adapted membrane (partially reduced $F_{A/B}$); (E) 10 mM sodium dithionite, 5 min preillumination at 205 K (reduced $F_{A/B/X}$); (G) 10 mM sodium dithionite, 15 min preillumination at 220 K (reduced $F_{A/B/X}$, partially photoaccumulated A_1^{-}). Panels B, D, F, and H show the sine Fourier transforms (SFT) of the ESEEM shown in panels A, C, E, and G, respectively. Key: solid circles, SFT of the experimental results; solid lines, SFT of the fit functions. The dashed vertical lines indicate the positions of the canonical features in the ESEEM spectra at $\pm 2(J - 2D/3)$ and $\pm 2(J + D/3)$ calculated from the fit parameters reported in Table 2. Experimental conditions are as in the legend of Figure 4.

acceptors of PS I. A general increase in the value of the exchange interaction J occurs, from a value of 0.5−1 μT in samples in which the iron−sulfur centers are initially oxidized to a value of 3−4 μT in samples in which F_X is reduced and A_1 has been partially photoaccumulated. A parallel increase of the absolute value of the dipolar interaction energy D is observed. The maximum value of D of −(167−169) μT, equivalent to a distance between the radical pair partners of 25.5−25.3 Å, is obtained when $F_{A/B/X}$ are initially oxidized; this shifts to a minimum of −191.7 μT, equivalent to a distance of 24.4 Å, following almost complete reduction of A_{1A} in the spinach digitonin PS I preparation.

Previous OOP-ESEEM studies of the [$P_{700}^{+}A_1^{-}$] radical pair in site-directed mutants of the axial ligand of the primary acceptor A_0 in *C. reinhardtii* have led to the proposition that the two decay rates of the ESE are due to two radical pairs, one on the PsaA branch and the other on the PsaB branch of the PS I reaction center (*7*). The distances obtained from the OOP-ESEEM fits of [$P_{700}^{+}A_{1A}^{-}$] and [$P_{700}^{+}A_{1B}^{-}$] have been shown to be fully consistent with the X-ray structure (*7*) when the strong asymmetry of the spin distribution in P_{700}^{+} toward the PsaB-bound chlorophyll, as indicated by high-field EPR and ENDOR studies, is taken into account (*39*−*42*). The observation that the OOP-ESEEM recorded in wild-type *C. reinhardtii* thylakoids upon reduction of F_X can be reconstructed as a linear combination of the OOP-ESEEM detected in the PsaA-M684H and the PsaB-M664H mutants, in which the modulation associated with each radical pair can be selectively monitored, further confirms the bidirectional electron transfer hypothesis (*7*).

In conditions under which the terminal Fe−S clusters are initially oxidized, the estimates of the exchange and dipolar interactions are fully consistent in all of the samples under

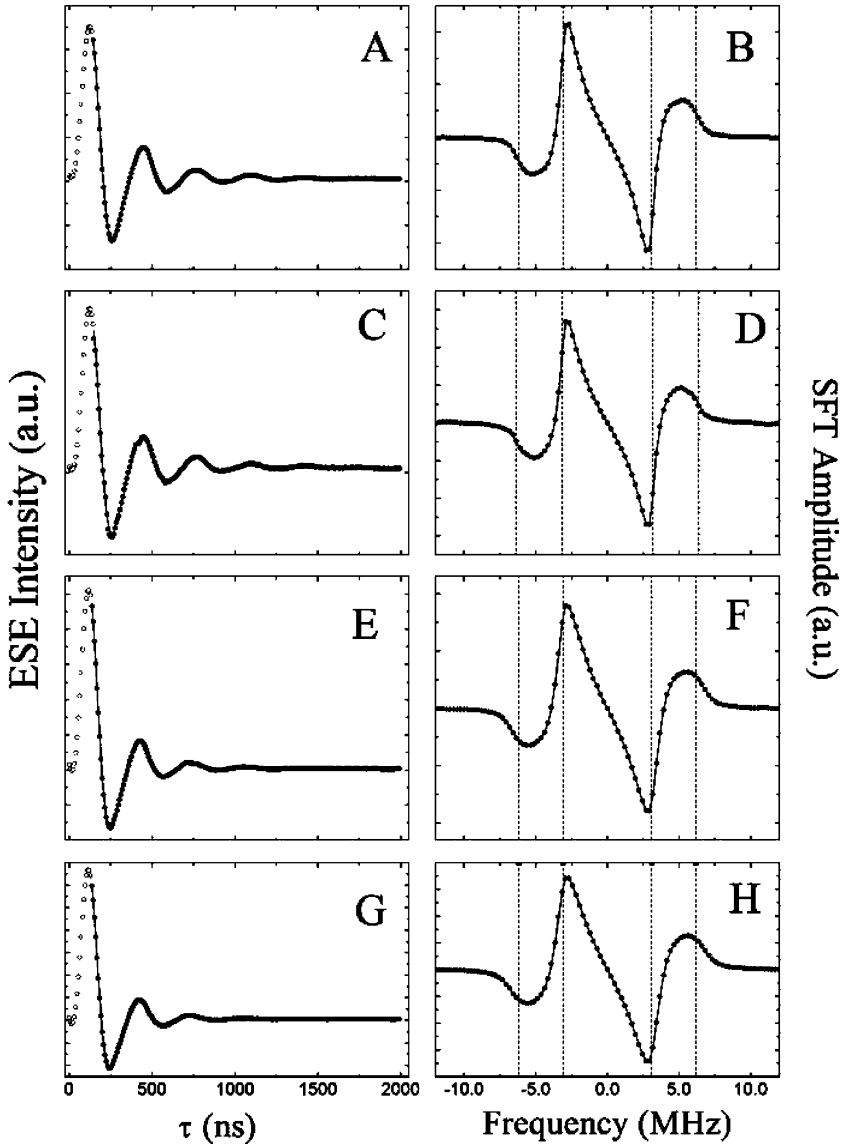

FIGURE 6: Time dependence of the out-of-phase ESEEM of the spin-correlated radical pair $[P_{700}{}^{+}A_1{}^{-}]$ in *Synechocystis* sp. PCC 6803 thylakoids. Solid circles are the experimental results; solid lines are the fits according to eq 1; open circles are the extrapolation to $\tau = 0$. Panels: (A) 20 mM sodium ascorbate, dark-adapted membrane (oxidized $F_{A/B/X}$); (C) 10 mM sodium dithionite, 5 min preillumination at 205 K (reduced $F_{A/B/X}$); (E) 10 mM sodium dithionite, 15 min preillumination at 220 K (reduced $F_{A/B/X}$, partially photoaccumulated $A_1{}^{-}$); (G) 10 mM sodium dithionite, 30 min preillumination at 220 K (reduced $F_{A/B/X}$, partially photoaccumulated $A_1{}^{-}$). Panels B, D, F, and H show the SFT of the ESEEM shown in panels A, C, E, and G, respectively. Key: solid circles, SFT of the experimental results; solid lines, SFT of the fit functions. The dashed vertical lines indicate the positions of the canonical features as described in the legend of Figure 5. Experimental conditions are as in the legend of Figure 4.

investigation (Table 2). The fits yield values of J of 0.5−0.7 μT and D of −(167.15−169.32) μT, which in turn allows a distance determination of 25.4−25.5 Å. These values are in full agreement with the original estimates in *Synechococcus elongatus* PS I preparations and single crystals, for which values of $J = 1$ μT and $D = -170$ μT were determined, from which a distance between the spins in the radical pair of 25.5 Å can be inferred (*33*, *35*, *36*). Similar values were obtained for the PsaB-M664H mutant of *C. reinhardtii*, which shows an electron spin echo signal arising from $[P_{700}{}^{+}A_{1A}{}^{-}]$ only (*7*). The partial reduction of F_A and F_B by sodium dithionite induces an increase in the initial intensity of the OOP-ESE, a small increase in the fast component in the decay (lifetime ~2 μs), and a parallel shift in the ESEEM modulation frequency. The change in the modulation frequency, and therefore in the estimated values of D and J, is rather modest, but still significant, in spinach and *C. reinhardtii* thylakoids and somewhat more evident in the spinach PS I digitonin preparation (Table 2).

After a brief preillumination at 205 K, which leads to a complete reduction of the terminal clusters $F_{A/B}$ and a significant reduction of F_X, the OOP-ESEEM recorded using thylakoids and cellular membranes from different species and the digitonin PS I preparation from spinach yield consistent results. There is a large increase in the amplitude of the fast decaying component of the ESE signal and a significant change in the frequency of the OOP-ESEEM. The value of J is 1−2 μT and D is in the range −(174−181) μT, which in turn leads to a distance between the radicals of 24.8−25.2 Å (Table 2).

Progressive preillumination at 205 K (data not presented) or 220 K (Figures 4−6, Table 2) results in a systematic change in the proportions of the fast and slow phases of the ESE signal decay and a change in the modulation frequency

Table 2: Fit Parameters for the Out-of-Phase ESEEM of the Radical Pair $[P_{700}^{+}A_{1}^{-}]$[a]

	D (μT)	J (μT)	T (μs)	distance (Å)
spinach thylakoids				
Asc, dark	-168.63 ± 0.42	0.31 ± 0.20	0.4145 ± 0.0054	25.47 ± 0.02
Dit, dark	-169.88 ± 0.15	1.61 ± 0.27	0.4043 ± 0.0020	25.41 ± 0.01
Dit, 5 min (205 K)	-174.01 ± 0.48	1.68 ± 0.25	0.3825 ± 0.049	25.20 ± 0.02
Dit, 15 min (220 K)	-186.03 ± 0.50	3.20 ± 0.23	0.3526 ± 0.038	24.65 ± 0.02
spinach PS I enriched membranes				
Asc, dark	-169.24 ± 0.58	1.37 ± 0.27	0.4349 ± 0.0076	25.44 ± 0.03
Dit, dark	-172.03 ± 0.54	2.36 ± 0.26	0.3802 ± 0.0044	25.30 ± 0.03
Dit, 5 min (205 K)	-181.12 ± 0.58	2.94 ± 0.29	0.3197 ± 0.0044	24.87 ± 0.03
Dit, 15 min (220 K)	-191.68 ± 0.54	4.31 ± 0.27	0.2971 ± 0.0034	24.40 ± 0.03
C. reinhardtii thylakoids				
Asc, dark	-169.32 ± 0.60	0.51 ± 0.18	0.6021 ± 0.014	25.43 ± 0.03
Dit, dark	-170.29 ± 0.58	1.28 ± 0.38	0.5872 ± 0.014	25.39 ± 0.03
Dit, 5 min (205 K)	-178.39 ± 0.41	2.28 ± 0.20	0.3883 ± 0.0047	25.00 ± 0.02
Dit, 15 min (220 K)	-191.70 ± 0.38	4.49 ± 0.22	0.3332 ± 0.0067	24.40 ± 0.02
Synechocystis sp. PCC 6803 thylakoids				
Asc, dark	-167.15 ± 0.41	1.03 ± 0.20	0.4134 ± 0.0047	25.54 ± 0.02
Dit, 5 min (205 K)	-172.09 ± 0.43	1.65 ± 0.33	0.3928 ± 0.0052	25.20 ± 0.03
Dit, 15 min (205 K)	-175.96 ± 0.46	1.99 ± 0.22	0.3723 ± 0.0049	25.10 ± 0.02
Dit, 30 min (220 K)	-177.57 ± 0.29	2.12 ± 0.12	0.3113 ± 0.0075	25.03 ± 0.01

[a] Results of fitting the ESEEM associated with the spin-polarized radical pair $[P_{700}^{+}A_{1}^{-}]$ in thylakoid membranes from the several different organisms as a function of the reduction state of electron transfer acceptors in photosystem I. Abbreviations have the same meaning as in the legend of Table 1.

of the OOP-ESEEM and, therefore, in the value of the spin−spin interaction energies within $[P_{700}^{+}A_{1}^{-}]$. However, for equivalent preillumination times at 220 K, different preparations show different changes of the OOP-ESEEM frequency. The PS I digitonin preparation exhibits the most marked response to the treatment, while the *Synechocystis* cellular membranes show the least. The OOP-ESEEM time dependences obtained for *Synechocystis* are therefore presented for longer illumination times of 15 and 30 min. Spinach and *C. reinhardtii* thylakoids show a similar intermediate response to the preillumination treatment (Table 2). The shift in the frequency modulation of the OOP-ESEEM parallels the quenching of the absolute amplitude associated with the $\sim$15−20 μs component of the OOP electron spin echo decay. As previously discussed and shown in Figure 3, this is associated with the photoaccumulation of A_{1A}, which is more readily achieved in the digitonin PS I spinach preparations than in thylakoids.

We interpret the experimental observations as showing that, after reduction of $F_{A/B/X}$, the modulation of the OOP-ESEEM originates from a superposition of two basic modulation frequencies arising from the radical pairs $[P_{700}^{+}A_{1A}^{-}]$ and $[P_{700}^{+}A_{1B}^{-}]$ populated one on each branch of the reaction center. The two species are characterized by different sets of spin−spin interaction energies as a result of the asymmetric spin delocalization on the Chl dimer constituting P_{700}^{+} (*39*−*42*). Photoaccumulation of the phylloquinone on the PsaA subunit (A_{1A}) leads to a progressive suppression of the modulation associated with the $[P_{700}^{+}A_{1A}^{-}]$ radical pair, so that different proportions of the modulations associated with $[P_{700}^{+}A_{1A}^{-}]$ and $[P_{700}^{+}A_{1B}^{-}]$ are observed, resulting in the detected shift in the ESEEM modulation frequency in the photoaccumulated samples.

If that is the case, the observed OOP-ESEEM signals should be the sum of two model functions of the form of eq 1. We have therefore performed a global fitting analysis of the ESEEM data acquired for different reduction states of the terminal acceptors of PS I using a linear combination of fit functions (eq 3). The values of the global variables D and J determined in the PsaA-M684H and the PsaB-M664H mutants of *C. reinhardtii* have been used as initial estimates. The results of this analysis for thylakoid preparations from the different organisms, recorded under conditions where F_X is essentially fully reduced, are shown in Figure 7. The complete set of fit parameters is listed in Table 3. It can be seen that the fits of the ESEEM data are excellent and that only a slight change in the values of D and J from the initial estimates [$D = -194.84$ μT, $J = 4.59$ μT and $D = -171.02$ μT, $J = 0.80$ μT, derived from the OOP-ESEEM of the PsaA-M684H and the PsaB-M664H mutants of *C. reinhardtii* (*7*)] is needed to describe the experiments. As an example we will discuss the case of spinach thylakoids. When the thylakoids are incubated with sodium ascorbate (not shown) or sodium dithionite in the dark, the OOP-ESEEM signals are dominated by the modulation characterized by the interactions $D = -168.50$ μT and $J = 0.31$ μT which we interpret as arising from the $[P_{700}^{+}A_{1A}^{-}]$ radical pair. The modulation component with $D = -194.79$ μT and $J = 4.24$ μT, associated with $[P_{700}^{+}A_{1B}^{-}]$, contributes in this case less than 30% of the ESEEM signal. As a result of reduction of F_X the fractional amplitudes of the two modulations become almost identical. Similar results were obtained in *C. reinhardtii* thylakoids, but $[P_{700}^{+}A_{1B}^{-}]$ becomes predominant in the spinach PS I preparation while it is still a minor component ($\sim$35%) in *Synechocystis* cellular membranes. In samples in which the A_{1A}^{-} phyllosemiquinone has been progressively photoaccumulated, the fractional amplitude of the modulation associated with $[P_{700}^{+}A_{1B}^{-}]$ increases and becomes dominant, in all samples except *Synechocystis* cellular membranes, after 30 min of preillumination at 220 K. However, also in *Synechocystis*, the modulation with $D = -191.38$ μT and $J = 3.87$ μT accounts for about 60% of the total ESEEM amplitude, indicating that the radical pair on the PsaB subunit is significantly populated in this organism as well. Even though there is not a strict numerical correlation, the relative weights associated with the two model fit functions, which are interpreted as the relative contributions of $[P_{700}^{+}A_{1A}^{-}]$ and $[P_{700}^{+}A_{1B}^{-}]$, show a similar

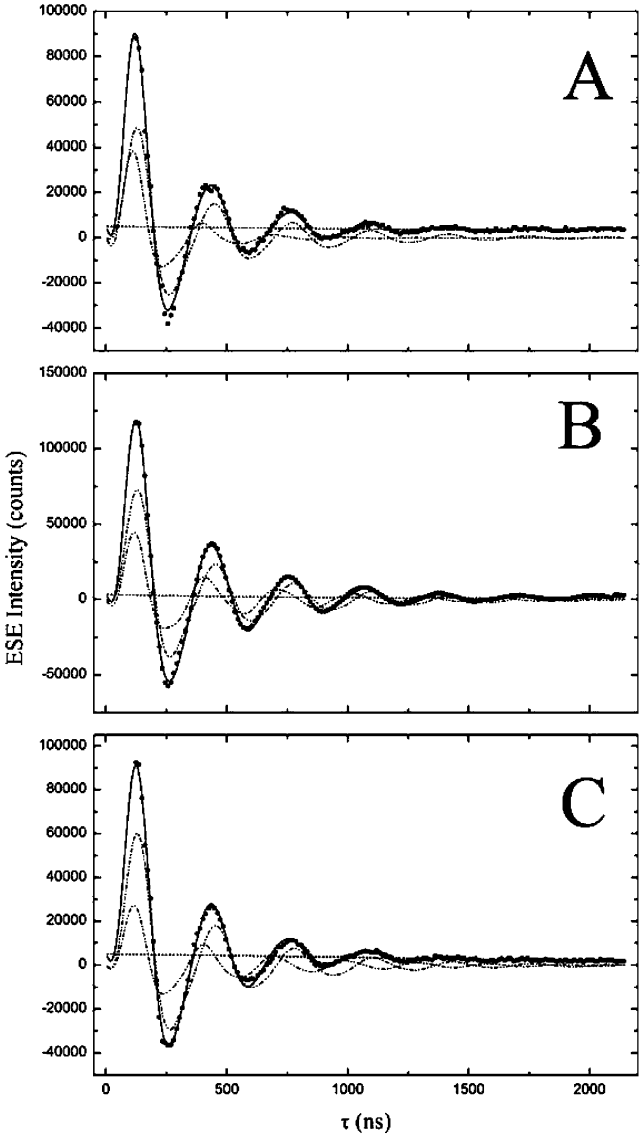

FIGURE 7: Global fitting of the time dependences of the out-of-phase ESEEM of the spin-correlated radical pair $[P_{700}^{+}A_1^{-}]$ by a combination of two ESEEM fit functions. Results are shown for thylakoid membranes incubated in 10 mM sodium dithionite and after 5 min preillumination at 205 K (reduced $F_{A/B/X}$). Key: open circles, experimental results; dash−dotted lines, graph of each of the ESSEM time dependences that, as a sum (solid line), describe the experimental results; dash−dotted line, quadratic baseline correction. The fit function (solid line) is extrapolated to $\tau = 0$. Panels: (A) spinach thylakoids; (B) *C. reinhardtii* thylakoids; (C) *Synechocystis* sp. PCC 6803 thylakoids. Experimental conditions are as in the legend of Figure 4.

trend and are in general qualitative agreement with the relative amplitudes of the ∼2−4 and ∼15−20 μs components of the ESE decay, which are also interpreted as being associated with the radical pairs on the two PS I reaction center subunits. The interpretation of the experimental results is fully consistent with the investigation by high-field/high-frequency (D-band) EPR of Poluektov et al. (*58*). Two different spin-polarized EPR spectra were recorded in cells of *Synechococcus lividus* (*58*) under conditions in which the Fe-S cluster is initially oxidized and after complete photoaccumulation of A_{1A}^{-}. The analysis of the two radical pairs is consistent with the geometry and spin−spin interaction values proposed for the $[P_{700}^{+}A_{1A}^{-}]$ and $[P_{700}^{+}A_{1B}^{-}]$ radical pairs (*58*), as originally proposed from the investigation of site-directed mutants of *C. reinhardtii*.

The data obtained here in wild-type samples from different organisms which are considered as representative models for evolutionarily divergent phyla (i.e., higher plants, green algae, and cyanobacteria) are consistent with the original interpretation of the data obtained in *C. reinhardtii* (*7*) and indicate that bidirectional electron transfer is a general characteristic of PS I electron transfer in all types of oxygenic photosynthetic organisms. The value of the interspin distance between P_{700}^{+} and A_{1A}^{-} has an average value of 25.45 Å and a small variation of 0.2 Å among the species investigated (Table 3). Similarly, the spin−spin distance between P_{700}^{+} and A_{1B}^{-} is 24.33 Å with a dispersion of about 0.1 Å. These observations should be taken as an indication that the structure of the PS I reaction center is extremely conserved during evolution, as suggested by structural studies in higher plants and cyanobacteria (*2*, *3*).

Our data seem to indicate that, at least at low temperature, PS I reaction centers are frozen in conformational states which favor electron transfer either along the PsaA or along the PsaB subunit. This can be inferred from both the increase of the ESE amplitude as a result of F_X prereduction and the reduced amplitude of the ESE following A_{1A}^{-} photoaccumulation without apparent redistribution toward the PsaB side electron transfer branch (Figure 2). Heterogeneity of conformers in PS I reaction centers has been previously reported in respect of the primary donor triplet state $^3P_{700}$ monitored by optically detected magnetic resonance, both in purified PS I particles and in thylakoids and leaves (*59*−*62*). However, the molecular details and physiological significance of the two conformational bands attributed to $^3P_{700}$ are still to be determined. So far, there is no evidence that they originate from recombination of radical pairs populated either on the PsaA or on the PsaB subunits.

Moreover, the measurements presented in this study are performed at 100 K where charge recombination is observed. Although at this temperature the system seems to be frozen in different conformational states, this situation might differ significantly at room temperature when a larger degree of conformational freedom is present and redistribution of the fraction of electrons transferred between the two electron transfer branches might occur. The extent to which electron transfer is directed to each side of the reaction center under physiological conditions and the factors determining the control of directionality in individual reaction centers remain to be determined unambiguously. In a recent study (*20*) it has been reported that symmetrical mutations of the A_0 binding site led to an apparent redistribution of the two kinetic phases of A_1^{-} reoxidation at room temperature. The data were interpreted as suggesting that the effect of the mutations is to modify the reaction center so as to favor electron transfer through one or the other electron transfer branch (*20*). However, in the experiments by Li et al. (*20*) an absolute quantification of the A_1^{-} reoxidation rates is not possible because the experiments are performed in entire cells. Thus, due to light scattering, sieve, and flattening effects, it is impossible to quantify the optical bleaching in terms of absolute extinction coefficients. Thus no absolute

Table 3: Global Fitting of the Out-of-Phase ESEEM of the Radical Pair [$P_{700}^+A_1$] Using a Linear Combination of Two ESEEM Fit Functions[a]

	D (μT)	J (μT)	distance (Å)	Dit, dark		Dit, 5 min (205 K)		Dit, 15 min (220 K)		Dit, 30 min (220 K)	
				T (μs)	A_i	T (μs)	A_i	T (μs)	A_i	T (μs)	A_i
spinach thylakoids											
$S_1(\tau)$	−168.50 ± 2.81	0.31 ± 0.33	25.48 ± 0.14	0.480 ± 0.008	0.709 ± 0.016	0.490 ± 0.010	0.596 ± 0.020	0.432 ± 0.015	0.299 ± 0.034	0.413 ± 0.012	0.044 ± 0.041
$S_2(\tau)$	−194.79 ± 3.42	4.24 ± 0.42	24.27 ± 0.14	0.326 ± 0.010	0.291 ± 0.012	0.313 ± 0.007	0.404 ± 0.014	0.309 ± 0.014	0.701 ± 0.022	0.308 ± 0.009	0.956 ± 0.032
spinach PS I enriched membranes											
$S_1(\tau)$	−168.28 ± 2.81	0.55 ± 0.33	25.49 ± 0.14	0.507 ± 0.020	0.628 ± 0.025	0.485 ± 0.010	0.318 ± 0.022	0.412 ± 0.013	0.255 ± 0.044	0.403 ± 0.015	0.140 ± 0.054
$S_2(\tau)$	−193.65 ± 2.29	4.18 ± 0.61	24.32 ± 0.10	0.335 ± 0.018	0.371 ± 0.024	0.324 ± 0.012	0.682 ± 0.018	0.300 ± 0.009	0.765 ± 0.033	0.288 ± 0.011	0.950 ± 0.043
C. reinhardtii thylakoids											
$S_1(\tau)$	−167.68 ± 2.47	0.65 ± 0.45	25.52 ± 0.13	0.602 ± 0.025	0.877 ± 0.078	0.585 ± 0.029	0.616 ± 0.079	0.566 ± 0.042	0.213 ± 0.013	0.546 ± 0.032	0.041 ± 0.055
$S_2(\tau)$	−193.46 ± 2.07	5.44 ± 0.61	24.33 ± 0.09	0.324 ± 0.018	0.123 ± 0.081	0.325 ± 0.022	0.384 ± 0.061	0.318 ± 0.032	0.717 ± 0.024	0.308 ± 0.042	0.959 ± 0.063
Synechocystis PPC 6803 thylakoids											
$S_1(\tau)$	−167.97 ± 2.20	0.65 ± 0.74	25.30 ± 0.11	0.444 ± 0.033	0.815 ± 0.051	0.442 ± 0.029	0.735 ± 0.089	0.469 ± 0.010	0.469 ± 0.035	0.395 ± 0.016	0.413 ± 0.052
$S_2(\tau)$	−191.38 ± 2.58	3.87 ± 0.61	24.42 ± 0.11	0.298 ± 0.032	0.185 ± 0.031	0.288 ± 0.042	0.265 ± 0.061	0.277 ± 0.023	0.531 ± 0.032	0.264 ± 0.014	0.587 ± 0.065

[a] Results of global fitting the ESEEM associated with the spin-polarized radical pair [$P_{700}^+A_1^-$] using a combination of two fit functions in thylakoid membranes from the several different organisms as a function of the reduction state of electron transfer acceptors in photosystem I. The data have been fitted using eq 3 with the ESEEM modulation parameters constrained to be the same for all of the acceptor reduction conditions, while the weighting factors A_i were allowed to change. Abbreviations have the same meaning as in the legend of Table 1.

estimate of electrons transferred through each electron branch can be unambiguously computed. Moreover, the results of ref *20* can be interpreted in the frame of the reversible charge separation model, originally proposed by Holzwarth and co-workers (*63*−*65*) and more recently implemented to include the entire set of electron transfer reactions in PS I (*66*). It is generally accepted that the effect of mutations at the level of A_0 the axial or hydrogen bond donor is to lengthen the lifetime of the [$P_{700}^+A_0^-$] radical pair (*10*, *15*, *16*). This is probably due to the fact that the redox potential of A_0 becomes more negative. As a result, the driving force of the reaction is reduced and the rate of the back-reaction becomes competitive with the forward electron transfer rate as the equilibrium constant is governed by the Boltzmann distribution. Thus, electron transfer reactions occurring on the unperturbed electron transfer chain are favored, which is in agreement with our previous electron transfer calculations (*66*). Neither the electron transfer calculations (*66*) nor the results of Li and co-workers (*20*) are in disagreement with the results reported here measured at cryogenic temperatures, where a large inhomogeneity of reaction center conformations has been observed and analyzed (*19*, *23*). This is because at room temperature there is enough thermal energy so that a dynamic distribution exists in which each reaction center is essentially in thermodynamical equilibrium with its possible conformers. On the other hand, in the frozen state, the centers could be trapped in different conformational states, some of which would favor electron transfer either on the PsaA- or on the PsaB-bound cofactor chains.

Relation between the Recombination Rates and Exchange Coupling Energy. In the following we relate the measured rate of charge recombination to the available structural data, obtained by X-ray crystallography (*2*, *3*), and the spin−spin interaction parameters derived in the present study, in the framework of nonadiabatic electron transfer theory.

The rate of an electron transfer reaction can be expressed in terms of the Marcus equation when contributions from molecular and solvent (protein) modes are neglected:

$$k_{et} = \frac{2\pi|V_{ab}|^2}{\sqrt{4\pi\lambda_t k_B T}} \exp\left[-\frac{(\lambda_t + \Delta G^\circ)^2}{4\lambda_t k_B T}\right] \quad (4)$$

where V_{ab} is the electronic coupling matrix element, λ_t is the (total) reorganization energy, ΔG° is the standard Gibbs free energy difference between the electron donor and acceptor, k_B is the Boltzmann constant, and T is the absolute temperature (*67*, *68*).

Charge recombination between P_{700}^+ and A_1^- is biphasic: lifetimes of ∼10−20 and ∼150−350 μs have been reported using transient optical spectroscopy (*23*−*25*), while EPR gives ∼2−4 and ∼15−20 μs (Table 1 and refs *4* and *7*). The discrepancy is due to the fact that loss of spin coherence in the radical pair state contributes to the decay of the spin-polarized [$P_{700}^+A_1^-$] EPR signal but not to the decays measured in optical experiments. In both cases the amplitudes of the "slow" and the "fast" components are in the ratio ∼2:1. Because the rates of magnetic relaxation are about 1 order of magnitude larger than the rates of charge recombination, in the following we will initially limit the discussion to the values reported in transient optical measurements of the charge recombination reaction.

Schlodder et al. (*23*) found that the slow 200 μs recombination component is essentially temperature independent. This result is expected in the case that $\Delta G^\circ \approx -\lambda_t$. This is not unreasonable given the redox potential of P_{700}^+ (∼470−500 mV) and that of $A_{1A}^- \sim -(600-700)$ mV (*66*) and a reorganization energy of about 1 eV (*21*). We have recently shown that the electron transfer reaction in PS I can be modeled assuming almost equipotential phylloquinones on the two reaction center branches (*56*). The estimated difference in redox midpoint potentials is 10−40 mV. Therefore,

one would expect the recombination on both electron transfer branches to show only modest temperature dependencies. Hence the rate of electron transfer would be determined principally by the electronic coupling V_{ab} in eq 4.

Although an accurate value for V_{ab} can in principle be obtained from the crystallographic data, this is notoriously difficult. Alternative strategies to obtain information about V_{ab} involve an analysis of electron transfer rates and the magnitude of the exchange interaction energy J which is, to a first approximation, proportional to the value of $|V_{ab}|^2$ (*69*−*71*).

The value of the electronic coupling responsible for electron transfer exhibits an approximately exponential dependence on the separation of the donor and acceptor molecules:

$$|V_{ab}|^2 = |V_0|^2 \exp(-\beta X^*_{ab}) \quad (5)$$

where V_0 is the value of V_{ab} when the donor and acceptor are in contact, X^*_{ab} is the edge-to-edge separation of the donor and acceptor, and β is the tunneling parameter. Dutton and Moser (*72*) proposed an "average" value for β of 1.4 $Å^{-1}$ from an analysis of various proteins involved in electron transfer The edge-to-edge distances between the Chl *a*′, which was shown to carry most of the spin density in P_{700}^+ (*39*−*42*), and the two phylloquinones bound to the PsaA and the PsaB reaction center subunits are 19.25 and 17.25 Å, respectively. Using the semiempirical relation $\log k_{et}^{RT} = 15 - 0.6X^*_{ab} - 3.1[(\Delta G° + \lambda_t)^2/\lambda_t]$, we obtain values for the two recombination rates of 350 and 22 μs. The ratio of the two rates is 15, which is close to that obtained experimentally by optical methods. It should be noted that a similar ratio is also observed in the decay of the spin-polarized $[P_{700}^+A_1^-]$ radical pair by magnetic resonance techniques, although the interpretation is complicated by magnetic relaxation phenomena.

As a first approximation let us assume that J has the same distance dependence as $|V_{ab}|^2$. We can then write

$$J_{X_2}/J_{X_1} = \exp(-\beta[X_2 - X_1]) \quad (6)$$

where J_{X_i} is the exchange interaction of a radical pair with separation X_i. If we now consider the experimental values of J and the associated Cramer−Rao lower bounds $J_{X_1} = 4.59 \pm 0.22$ μT and $J_{X_2} = 0.5 \pm 0.2$ μT, estimated in ref *7* for the site-directed mutants of *Chlamydomonas* (see also the global fitting results in Table 3), which were interpreted as showing modulation arising from two radical pair states populated on each reaction center subunit selectively, the ratio J_{X_1}/J_{X_2} lies between 6.8 and 14.5, with an average value of 9.2, which shows sensible agreement with the experimental values.

The Moser−Dutton correlation between the electronic coupling and the donor−acceptor distance can only be considered as a first approximation, and the point-dipole approximation in the derivation of the analytical formula that describes the ESEEM modulation is also not perfect. There also is no strong argument to expect J to have *exactly* the same distance dependence as the electronic coupling that controls the electron transfer. Despite these factors there is surprisingly good agreement between predicted and observed values of J_{X_1}/J_{X_2}, the measured electron transfer rate, and physical edge-to-edge distances derived from the crystal structure.

Finally, we will briefly consider the rates measured by EPR spectroscopy. The measured decay lifetime can be described as $\tau_m = (k_{cr} + k_{mr})^{-1}$, where k_{cr} is the rate of charge recombination and k_{mr} is the rate of magnetic relaxation. From the values of charge recombination kinetics, k_{mr} can be estimated as 2−5 μs^{-1} for the $[P_{700}^+A_{1B}^-]$ and 18−23 μs^{-1} for the $[P_{700}^+A_{1A}^-]$ radical pairs, respectively. These relaxation rates are 1.5−15 times faster than the recombination rates, and thus they strongly contribute to the decay rates of the spin-correlated $[P_{700}^+A_1^-]$ radicals monitored by the OOP-ESE. The difference in relaxation rates observed in the two radical pairs is probably related to the interaction of the phylloquinones with their binding sites, because the local environment of the Chl *a*′ which carries most of spin distribution in P_{700}^+ (*39*−*42*), is shared by both radical pairs. However, at present, it is not possible quantitatively or mechanistically to describe the processes which lead to different rates of relaxation.

CONCLUSION

We conclude that the results presented in this study are consistent with electron transfer occurring on both branches of the PS I reaction center subunits in all of the organisms investigated. The results, however, do not indicate the exact ratio between the amounts of electron density transferred along each side of the reaction center at room temperature, which may vary in different organisms or under different growth conditions.

SUPPORTING INFORMATION AVAILABLE

Two figures showing decay of the two-pulse electron spin echo associated with the radical pair $[P_{700}^+A_1^-]$ and the relationship between photoaccumulation treatment time and amplitudes of decay components of ESE associated with the $[P_{700}^+A_1^-]$ radical pair. This material is available free of charge via the Internet at http://pubs.acs.org.

REFERENCES

1. Heathcote, P. (2002) *Biochim. Biophys. Acta 1507*, 1−312.
2. Jordan, P., Fromme, P., Klukas, O., Witt, H. T., Saenger, W., and Krauss, N. (2001) Three-dimensional structure of cyanobacterial photosystem I at 2.5 angstrom resolution, *Nature 411*, 909−917.
3. Ben-Shem, A., Frolow, F., and Nelson, N. (2003) Crystal structure of plant photosystem I, *Nature 426*, 630−635.
4. Muhiuddin, I. P., Heathcote, P., Carter, S., Purton, S., Rigby, S. E. J., and Evans, M. C. W. (2001) Evidence from time-resolved studies of the $P700^{\bullet+}/A^{\bullet-}$ radical pair for photosynthetic electron transfer on both the PsaA and PsaB branches of the photosystem I reaction centre, *FEBS Lett. 503*, 56−60.
5. Rigby, S. E. J., Muhiuddin, I. P., Evans, M. C. W., Purton, S., and Heathcote, P. (2002) Photoaccumulation of the PsaB phyllosemiquinone in photosystem I of *Chlamydomonas reinhardtii*, *Biochim. Biophys. Acta 1556*, 13−20.
6. Fairclough, W. V., Forsyth, A., Evans, M. C. W., Rigby, S. E. J., Purton, S., and Heathcote, P. (2003) Bidirectional electron transfer in photosystem I: electron transfer on the PsaA side is not essential for phototrophic growth in *Chlamydomonas*, *Biochim. Biophys. Acta 1606*, 43−55.
7. Santabarbara, S., Kuprov, I., Fairclough, W., Hore, P. J. Purton, S., Heathcote, P., and Evans, M. C. W. (2005) Bidirectional electron transfer in photosystem I: determination of two distances between P_{700}^+ and A_1^- in spin-correlated radical pairs, *Biochemistry 44*, 2119−2128.

8. Joliot, P., and Joiot, A. (1999) *In vivo* analysis of the electron transfer within photosystem I: Are the two phylloquinones involved?, *Biochemistry 38*, 11130−11136.
9. Guergova-Kuras, M., Boudreaux, A., Joliot, A., Joliot, P., and Redding, K. (2001) Evidence for two active branches for electron transfer in photosystem I, *Proc. Natl. Acad. Sci. U.S.A. 98*, 4437−4442.
10. Ramesh, V. M., Gibasiewicz, K., Lin, S., Bingham, S., and Webber, A. N. (2004) Bidirectional electron transfer in photosystem I: accumulation of A_0^- in A-side or B-side mutants of the axial ligand to chlorophyll A_0, *Biochemistry 43*, 1369−1375.
11. Purton, S., Stevens, D. R., Muhiuddin, I. P., Evans, M. C. W., Carter, S., Rigby, S. E. J., and Heathcote, P. (2001) Site-directed mutagenesis of PsaA residue W693 affects phylloquinone binding and function in the photosystem I reaction center of *Chlamydomonas reinhardtii*, *Biochemistry 40*, 2167−2175.
12. Boudreaux, B., MacMillan, F., Teutloff, C., Agalorov, R., Gu, F. F., Grimaldi, S., Bittl, R., Brettel, K., and Redding, K. (2001) Mutations in both sides of the photosystem I reaction center identify the phylloquinone observed by electron paramagnetic resonance spectroscopy, *J. Biol. Chem. 276*, 37299−37306.
13. Yang, F., Shen, G., Schluchter, W. M., Zybailov, B. L., Ganago, A. O., Vassiliev, I. R., Bryant, D. A., and Golbeck, J. H. (1998) Deletion of the PsaF polypeptide modifies the environment of the redox-active phylloquinone (A_1). Evidence for unidirectionality of electron transfer in photosystem I, *J. Phys. Chem. B 102*, 8288−8299.
14. Xu, W., Chitnis, P., Valieva, A., van der Est, A., Brettel, K., Guergova-Kuras, K., Pushkar, J., Zech, S. G., Stehlik, D., Shen, G., Zybailov, B., and Golbeck, J. H. (2003) Electron transfer in cyanobacterial photosystem I: II. Determination of forward electron transfer rates of site-directed mutants in a putative electron transfer pathway from A_0 through A_1 to F_X, *J. Biol. Chem., 278*, 27876−27887.
15. Cohen, R. O., Shen, G., Golbeck, J. H., Xu, W., Chitnis, P. R., Valieva, A. I., van der Est, A., Pushkar, Y., and Stehlik, D., (2004) Evidence for asymmetric electron transfer in cyanobacterial photosystem I: analysis of a methionine-to-leucine mutation of the ligand to the primary electron acceptor A_0, *Biochemistry 43*, 4741−4754.
16. Salikhov, K. M., Pushkar, Y. N., Golbeck, J. H., and Stehlik, D. (2003) Interpretation of the multifrequency transient EPR spectra of the $P_{700}^+A_0Q_K^-$ state in photosystem I particles with a sequential correlated radical pair model: wild-type versus A_0 mutants, *Appl. Magn. Res. 24*, 467−482.
17. Kandrashkin, Y. E., Salikhov, K. M., van der Est, A., and Stehlik, D. (1998) Electron spin polarisation in consecutive spin-correlated radical pairs: application to the short-lived and long-lived-precursor in type I photosynthetic reaction centres, *Appl. Magn. Res. 15*, 417−447.
18. Setif, P., and Brettel, K. (1993) Forward electron transfer from phylloquinone A_1 to iron−sulfur centers in spinach photosystem I, *Biochemistry 32*, 7846−7854.
19. Brettel, K. (1997) Electron transfer and arrangement of the redox cofactors in photosystem I, *Biochim. Biophys. Acta 1318*, 322−373.
20. Li, Y., van der Est, A., Lucas, M. G., Ramesh, V. M., Gu, F., Petrenko, A., Lin, S., Webber, A. N., Rappaport, F., and Redding, K. (2006) Directing electron transfer within photosystem I by breaking H-bonds in the cofactor branches, *Proc. Natl. Acad. Sci. U.S.A. 103*, 2144−2149.
21. Bautista, J. A., Rappaport, F., Guergova-Kuras, M., Cohen, R. O., Golbeck, J. H., Wang, J. Y., Beal, D., and Diner, B. A. (2005) Biochemical and biophysical characterization of photosystem I from phytoene desaturase and zeta-carotene desaturase deletion mutants of *Synechocystis* sp. PCC 6803: evidence for PsaA- and PsaB-side electron transport in cyanobacteria, *J. Biol. Chem. 280*, 20030−20041.
22. Agalarov, R., and Brettel, K. (2003) Temperature dependence of biphasic forward electron transfer from the phylloquinone(s) A1 in photosystem I: only the slower phase is activated, *Biochim. Biophys. Acta 1604*, 7−12.
23. Schlodder, E., Falkenberg, M., Gergeleit, M., and Brettel, K. (1998) Temperature dependence of forward and reverse electron transfer from A_1^-, the reduced secondary electron acceptor in photosystem I, *Biochemistry 37*, 9466−9476.
24. Brettel, K., and Golbeck, J. H. (1996) Spectral and kinetic characterization of electron acceptor A(1) in a photosystem I core devoid of iron-sulfur centers F_X, F_B and F_A, *Photosynth. Res. 45*, 183−193.
25. Shinkarev, V. P., Zybailov, B., Vassiliev I. R., and Golbeck, J. H. (2002) Modelling of the P_{700}^+ charge recombination kinetics with phylloquinone and plastoquinone-9 in the A_1 site of photosystem I, *Biophys. J. 83*, 2885−2897.
26. van der Est, A. (2003) Light-induced spin polarization in type I photosynthetic reaction centres, *Biochim. Biophys. Acta 1507*, 212−225.
27. van der Est, A., Prisner, T., Bittl, R., Fromme, P., Lubitz, W., Mobius, K., and Stehlik, D. (1997) Time-resolved X-, K-, and W-band EPR of the radical pair state $P_{700}^+A_1^-$ of photosystem I in comparison with $P_{865}^+Q_A^-$ in bacterial reaction centers, *J. Phys. Chem. B 101*, 1437−1443.
28. Pushkar, Y. N., Golbeck, J. H., Stehlik, D., and Zimmermann, H. (2004) Asymmetric hydrogen-bonding of the quinone cofactor in photosystem I probed by ^{13}C-labeled naphthoquinones, *J. Phys. Chem. B 108*, 9439−9448.
29. Salikhov, K. M., Kandrashkin, Y. E., and Salikhov, A. K. (1992) Peculiarity of the free induction and primary spin echo signal from spin-correlated radical pairs, *Appl. Magn. Res. 3*, 199−216.
30. Tang, J., Thurnauer, M. C., and Norris, J. R. (1994) Electron spin echo envelope modulation due to the exchange and dipolar interaction in a spin-correlated radical pair, *Chem. Phys. Lett. 219*, 283−290.
31. Hore, P. J., Hunter, D. A., McKie, C. D., and Hoff, A. J. (1987) Electron paramagnetic resonance of spin-correlated radical pairs in photosynthetic reaction centres, *Chem. Phys. Lett. 137*, 495−500.
32. Kothe, G., Weber, S. Ohmes, E., Thurnauer, M. C., and Norris, J. R. (1994) Transient EPR of light-induced radical pairs: manifestation of zero quantum coherence, *J. Chem. Phys. 98*, 2706−2712.
33. Bittl, R., and Zech, S. G. (1997) Pulsed EPR study of spin-coupled radical pairs in photosynthetic reaction centres: measurements of the distance between P_{700}^+ and A_1^- in photosystem I and between P_{685}^+ and Q_A^- in bacterial reaction centres, *J. Phys. Chem. B 101*, 1429−1436.
34. Fursman, C. E., and Hore P. J. (1999) Distance determination in spin-correlated radical pairs in photosynthetic reaction centres by electron spin echo envelope modulation, *Chem. Phys. Lett. 303*, 593−600.
35. Dzuba, S. A., Hara, H., Kawamori, A., Iwaki, M., Itoh, S., and Tsvetkov, Y. D. (1997) Electron spin echo of spin-polarised radical pairs in intact and quinone-reconstituted plant photosystem I reaction centres, *Chem. Phys. Lett. 264*, 238−244.
36. Bittl, R., Zech, S. G., Fromme, P., Witt, H. T., and Lubitz, W. (1997) Pulsed EPR structure analysis of photosystem I single crystals: localization of phylloquinone acceptor, *Biochemistry 26*, 12001−12004.
37. Coffman, R. E., and Buettner, G. R. (1979) A limit function for long-range ferromagnetic and antiferromagnetic superexchange, *J. Phys. Chem. 83*, 2387−2392.
38. Hoffmann, S. K., Hilczer, W., and Goslar. J. (1994) Weak long-distance superexchange interaction and its temperature variations in copper(II) compounds studied by single-crystal EPR, *Appl. Magn. Res. 7*, 289−321.
39. Rigby, S. E. J., Nugent, J. H. A., and O'Malley, P. J. (1994) ENDOR and special triple resonance studies of chlorophyll cation radicals in photosystem 2, *Biochemistry 33*, 10043−10050.
40. Krabben, L., Schlodder, E., Jordan, P., Carbonera, D., Giacometti, G., Lee, H., Webber, A. N., and Lubitz, W. (2000) Influence of the axial ligands on the spectral properties of P700 of photosystem I: A study of site-directed mutants, *Biochemistry 39*, 13012−13025.
41. Kass, H., Fromme, P., Witt, H. T., and Lubitz, W. (2001) Orientation and electronic structure of the primary donor radical cation P_{700}^+ in photosystem I: A single crystals EPR and ENDOR study, *J. Phys. Chem. B 105*, 1225−1239.
42. Petrenko, A., Maniero, A. L., van Tol, J., MacMillan, F., Li, Y., Brunel, L.-C., and Redding, K. (2004) A high-field EPR study of P_{700}^+ in wild-type and mutant photosystem I from *Chlamydomonas reinhardtii*, *Biochemistry 43*, 1781−1786.
43. Diner, B. A., and Wollman, F. A. (1980) Isolation of highly active photosystem II particles from a mutant of *Chlamydomonas reinhardtii*, *Eur. J. Biochem. 110*, 521−526.
44. Rogner, M., Nixon, P., and Diner, B. A. (1990) Purification and characterization of photosystem I and photosystem II core

complexes from wild-type and phycocyanin-deficient strains of the cyanobacterium *Synechocystis* PCC 6803, *J. Biol. Chem. 265*, 6189−6196.
45. Jennings, R. C., Garlaschi, F. M., Gerola, P. D., Etzion-Katz, R., and Forti, G. (1981) Proton induced grana formation in chloroplast. Distribution of chlorophyll-protein complexes and photosystem II, *Biochim. Biophys. Acta 638*, 100−107.
46. Boardman, N. K. (1970) Subchloroplast fragments: digitonin method, *Methods Enzymol. 23*, 268−276.
47. Heathcote, P. Hanley, J. A., and Evans, M. C. W. (1993) Double-reduction of A_1 abolishes the EPR signal attributed to A_1^-—evidence for C2 symmetry in the photosystem I reaction-centre, *Biochim. Biophys. Acta 1144*, 54−61.
48. Evans, M. C. W., Sihra, C. K., Bolton, J. R., and Cammack, R. (1975) Primary electron acceptor complex of photosystem I in spinach chloroplasts, *Nature 256*, 668−670.
49. Evans, M. C. W., Sihra, C. K., and Cammack, R. (1976) The properties of the primary electron acceptor in the photosystem I reaction centre of spinach chloroplasts and its interaction with P700 and the bound ferredoxin in various oxidation−reduction states, *Biochem. J. 158*, 71−77.
50. MacMillan, F., Hanley, J. A., van der Weerd, L., Knupling, M., Un, S., and Rutherford, A. W. (1997) Orientation of the phylloquinone electron acceptor anion radical in photosystem I, *Biochemistry 36*, 9297−9303.
51. Hanley, J., Deligiannakis, Y., MacMillan, F., Bottin, H., and Rutherford, A. W. (1997) ESEEM study of the phyllosemiquinone radical A_1^- in ^{14}N- and ^{15}N-labeled photosystem I, *Biochemistry 36*, 11543−11549.
52. Vassiliev, I. R., Antonkine, M. L., and Goldbeck, J. H. (2001) Iron-sulphur clusters in type I reaction centres, *Biochim. Biophys. Acta 1507*, 139−160.
53. Chamorowsky, S. K., and Cammack, D. R. (1982) Direct determination of the midpoint potential of the acceptor X in chloroplast photosystem I by electrochemical reduction and electron spin resonance, *Photochem. Photobiophys. 4*, 195−200.
54. Parrett, K. G., Mehari, T., Warren, P. G., and Golbeck, J. H. (1989) Purification and properties of the intact P-700 and Fx-containing photosystem I core protein, *Biochim Biophys Acta 973*, 324−332.
55. Ke, B., Dolan, E., Sugahara, K., Hawkridge, F. M., Demeter, S., and Shaw, E. (1977) Photosynthetic organelles, *Plant Cell. Physiol.* (*Special Issue*), 187−199.
56. Moenne-Loccoz, P., Heathcote, P., MacLachlan, D. J., Berry, M. C., Davis, I. H., and Evans, M. C. W. (1994) Path of electron transfer in photosystem I—direct evidence of forward electron transfer from A_1 to $Fe-S_X$, *Biochemistry 33*, 10037−10042.18.
57. Rigby, S. E., Evans, M. C. W., and Heathcote, P. (1996) ENDOR and special triple resonance spectroscopy of A_1^- of photosystem I, *Biochemistry 35*, 6651−6656.
58. Poluektov, O. G., Paschenko, S. V., Utschig, L. M., Lakshmi, K. V., and Thurnauer, M. C. (2005) Bidirectional electron transfer in photosystem I: direct evidence from high-frequency time-resolved EPR spectroscopy, *J. Am. Chem. Soc. 127*, 11910−11911.
59. Searle, G. W., and Schaafsma, T. J. (1992) Fluorescence detected magnetic resonance of the primary donor and inner core antenna chlorophyll in photosystem I reaction centres protein: sign inversion and energy transfer, *Photosynth. Res. 32*, 193−206.
60. Carbonera, D., Collareta, P., and Giacometti, G. (1997) The P700 triplet state in intact environment, *Biochim. Biophys. Acta 1322*, 115−128.
61. Santabarbara, S., Bordignon, E., Jennings, R. C., and Carbonera, D. (2002) Chlorophyll triplet states associated with photosystem II of thylakoids, *Biochemistry 41*, 8184−8194.
62. Santabarbara, S., Jennings, R. C., and Carbonera, D. (2003) Analysis of photosystem II triplet states in thylakoids by fluorescence detected magnetic resonance as a function of the reduction state of the primary quinone acceptor Q_A, *Chem. Phys. 294*, 257−267.
63. Muller, M. G., Niklas, J., Lubitz, W., and Holzwarth, A. R. (2003) Ultrafast transient absorption studies on photosystem I reaction centers from *Chlamydomonas reinhardtii*. 1. A new interpretation of the energy trapping and early electron transfer steps in photosystem I, *Biophys. J. 85*, 3899−3922.
64. Holzwarth, A. R., Muller, M. G., Niklas, J., and Lubitz, W. (2005) Charge recombination fluorescence in photosystem I reaction centers from *Chlamydomonas reinhardtii*, *J. Phys. Chem. B 109*, 5903−5911.
65. Holzwarth, A. R., Muller, M. G., Niklas, J., and Lubitz, W. (2006) Ultrafast transient absorption studies on photosystem I reaction centers from *Chlamydomonas reinhardtii*. 2: mutations near the P700 reaction center chlorophylls provide new insight into the nature of the primary electron donor, *Biophys. J. 90*, 552−565.
66. Santabarbara, S., Heathcote, P., and Evans, M. C. W. (2005) Modelling of the electron transfer reactions in photosystem I by electron tunnelling theory: the phylloquinones bound to the PsaA and the PsaB reaction centre subunits of PS I are almost isoenergetic to the iron-sulphur cluster F_X, *Biochim. Biophys. Acta 1708*, 283−310.
67. Marcus, R. A., and Sutin, N. (1985) Electron transfer in chemistry and biology, *Biochim. Biophys. Acta 811*, 265−322.
68. DeVault, D. (1980) Quantum mechanical tunnelling in biological systems, *Q. Rev. Biophys. 13*, 387−564.
69. Okamura, M. Y., Isaacson, R. A., and Feher, G. (1979) Spectroscopic and kinetic properties of the transient intermediate acceptor in reaction centers of *Rhodopseudomonas sphaeroides*, *Biochim. Biophys. Acta 546*, 394−417.
70. Bixon, M., Jortner, J., Michel-Beyerle, M.-E., and Ogrodnik, A. (1989) A superexchange mechanism for the primary charge separation in photosynthetic reaction centers, *Biochim. Biophys. Acta 977*, 273−286.
71. Di Valentin, M., Bisol, A., Agostini, G., Fuhs, M., Liddell, P. A., Moore, A. L., Moore, T. A., Gust, D., and Carbonera, D. (2004) Photochemistry of artificial photosynthetic reaction centers in liquid crystals probed by multifrequency EPR (9.5 and 95 GHz), *J. Am. Chem. Soc. 126*, 17074−17086.
72. Moser, C. C., and Dutton, P. L. (1992) Engineering protein structure for electron transfer function in photosynthetic reaction centers, *Biochim. Biophys. Acta 1101*, 171−176.

BI060330H